

**Recent Syntheses and Biological Profiling of Quassinoids**

Journal:	<i>Organic & Biomolecular Chemistry</i>
Manuscript ID	OB-REV-03-2022-000490.R1
Article Type:	Review Article
Date Submitted by the Author:	26-Apr-2022
Complete List of Authors:	Pazur, Ethan; University of Pittsburgh, Department of Chemistry Wipf, Peter; University of Pittsburgh, Department of Chemistry

Recent Syntheses and Biological Profiling of Quassinoids

Ethan J. Pazur^a and Peter Wipf^{a,b}

Received 00th January 20xx,
Accepted 00th January 20xx

DOI: 10.1039/x0xx00000x

Quassinoid natural products have gained considerable recognition for their diverse biological properties and their synthetically challenging, highly oxygenated polycyclic structures. Herein, we discuss strategies and tactics in the total synthesis of quassinoids that were evolving over the past 15 years. Additionally, recent structure-activity relationships and potential biological mechanisms of actions are briefly summarized.

1. Introduction

Quassinoids comprise a group of over 160 secondary metabolites isolated from extracts of the *Simaroubacea* family of trees and bushes that grow in mostly tropical climate.¹ These highly oxygenated triterpenoids are structurally related to limonin (**2**), and feature fused and bridged rings flanked by a valerolactone (Figure 1). Quassinoids are categorized as C₁₈, C₁₉, C₂₀, C₂₂, C₂₅, and C₂₆ based on the number of backbone carbons, and most contain the picrasane ABCD-ring skeleton (**1**). Biosynthetically, they are believed to originate from the oxidation of tetracyclic terpenes; for example euphol (**3**).² Further oxidative cleavage generates the *seco-nor*-picrasane framework of the polyandranes (**4**).

Since their isolation and structural elucidation, quassinoids such as quassin (**5**) and brusatol (**7**) have been the subject of intensive biological and synthetic studies attributable to their potent biological properties.^{3–12} For example, the quassinoid bruceantin (**6**) has reached Phase II clinical trials for the

treatment of metastatic breast cancer and malignant melanoma in 1982 and 1983, respectively.^{13, 14} Although originally dismissed for its toxic side effects, bruceantin still appears to sustain potential as a viable drug candidate for several cancer types.¹⁵

Despite their significant anticancer, antiviral, insecticidal, and other bioactivities, the structural complexity, particularly the dense oxygenation and stereogenic carbon array of quassinoids has limited the number of successful total syntheses.^{16–19} However, many reports document the synthesis of advanced intermediates and showcase various methodologies that can access the tetra- or pentacyclic ring cores. This report will primarily focus on developments since 2005 that culminate in the total synthesis of quassinoids or contribute key new methods for the construction of significant substructural elements.



Ethan Pazur holds a B.S. (Hons) in Chemistry from Lake Superior State University. He is a Ph.D. candidate in Chemistry at the University of Pittsburgh under the direction of Dr. Peter Wipf. Ethan's research interests include natural product synthesis and medicinal chemistry.



Peter Wipf obtained a Dipl. Chem. and a PhD in Chemistry with Prof. Heinz Heimgartner from the Institute for Organic Chemistry at the University of Zürich. After a Swiss National Foundation Postdoctoral Fellowship at the University of Virginia with Prof. Robert E. Ireland, he joined the faculty at Pittsburgh, where he holds the rank of Distinguished University Professor. He is also currently a Visiting Professor at the University of Eastern Finland. His research interests include the total synthesis of natural products, heterocyclic and medicinal chemistry, and the discovery of new reactions with strained carbocycles.

^a Department of Chemistry, University of Pittsburgh, Pittsburgh, PA 15260, USA.

^b School of Pharmacy, University of Eastern Finland, FI-70210 Kuopio, Finland.

† Footnotes relating to the title and/or authors should appear here.

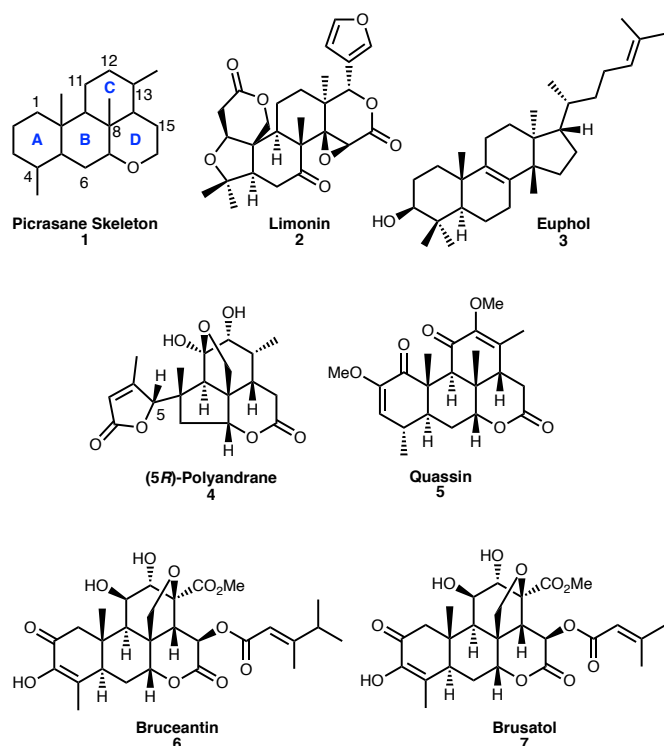


Figure 1 Representative Quassinoids and Structurally Related Natural Products

2. Total Syntheses of Quassinoids

2.1. (–)-Samaderine Y and Unnatural (–)-14-*epi*-Samaderine E

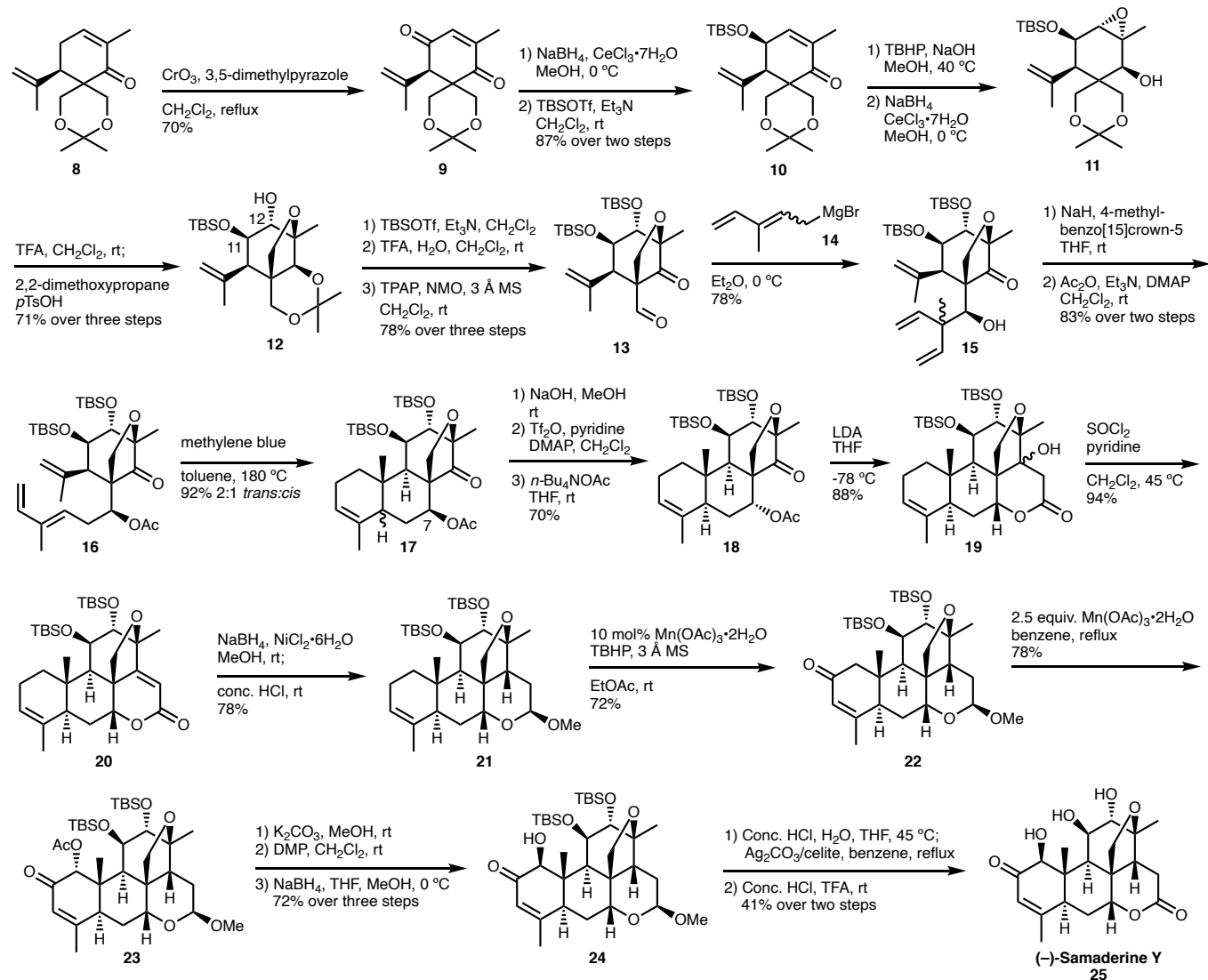
An efficient total synthesis of (–)-samaderine Y (**25**) was accomplished by Shing and Yeung in 2005. Starting with natural carvone, the target molecule was prepared in 21 steps and an impressive average yield of 81%/step.^{20, 21}

The construction of the fully oxygenated C-ring segment **12** of (–)-samaderine Y (**25**) was initiated from the carvone-derived intermediate **8** (Scheme 1). Allylic oxidation and selective Luche reduction of the less hindered carbonyl group in enedione **9** followed by silyl ether formation generated enone **10**. After treatment with *t*-butylhydroperoxide, the epoxyketone was reduced under Luche conditions to furnish epoxyalcohol **11**. Under anhydrous acidic conditions, an acetonide shift triggered the epoxide ring opening and the installment of the tetrahydrofuran bridge. A diol side product was then reprotected with 2,2-dimethoxypropane in the presence of *p*-toluenesulfonic acid to generate additional **12**.

The authors reasoned that the C-11 hydroxy group should be installed prior to construction of the tetrahydrofuran, based on previous efforts that proved difficult to achieve a C-11/C-12 diol through an elimination-dihydroxylation sequence.²² Presumably, the rigidity of the six-membered C-ring with a tetrahydrofuran bridge was disfavoring an intermediate with three consecutive *sp*²-carbons. In **12**, six stereogenic carbons (including an all-carbon quaternary center) and multiple functionalities could be leveraged for subsequent transformations.

After TBS-protection of the secondary alcohol in **12**, the acetonide was hydrolyzed and the diol oxidized with tetrapropylammonium perruthenate to give 1,3-dicarbonyl compound **13**. Pentadienyl Grignard **14** was used to append a diene to **13**, and an interesting oxyanion-accelerated [1,3]-sigmatropic rearrangement led to the conjugated diene suitable for the planned intramolecular Diels–Alder reaction (IMDA). After *O*-acetylation, diene **16** was heated in toluene at 180 °C in the presence of methylene blue as a radical inhibitor to provide tetracyclic **17** as an inseparable 2:1 mixture of diastereomers. Without further purification, this mixture was subjected to a 3-step sequence to invert the configuration at the C-7 acetate position to generate **18**. The introduction of the D-ring was initiated by an intramolecular aldol reaction of the acetate that gave lactone **19** as a mixture of diastereomers. Elimination of the tertiary alcohol produced the α,β -unsaturated lactone **20**, and reduction with nickel boride generated the saturated acetal **21** after addition of HCl to the solution of the lactol in methanol. A second allylic oxidation generated the A-ring enone **22**, and vigorous further oxidation installed the α -acetate to give **23**. The ester was cleaved with potassium carbonate in methanol, and a Dess–Martin periodinane (DMP) oxidation followed by selective reduction with sodium borohydride delivered the A-ring hydroxyketone **24** in high yield. Finally, a global deprotection and Fetizon oxidation afforded (–)-samaderine Y (**25**). While this synthesis proceeded in a linear fashion and required several oxidation/reduction steps, yields were uniformly high and the conversion of ketoaldehyde **13** to the tetracyclic **17** highlighted the efficiency of the IMDA method to rapidly expand molecular complexity.

Starting with intermediate **18**, unnatural (–)-14-*epi*-samaderine E (**30**) could be synthesized in 7 steps (Scheme 2).²¹ This sequence began with an allylic oxidation of **18** to give enone **26**. Next, α -acetoxylation led to α -acetate **27**, which possessed the incorrect stereochemistry at C-1 (analogous to what was observed during the total synthesis of (–)-samaderine Y). Inversion at this stereocenter was achieved through selective methanolysis of the C-1 acetate with potassium carbonate in methanol and subsequent DMP oxidation that led to the triketone. Next, diastereoselective reduction with sodium borohydride engendered **28**. Treatment of the acetate in **28** with lithium diisopropylamide (LDA) resulted in an intramolecular aldol reaction which gave the 14 α -hydroxy lactone **29** in 80% yield. The observed configuration was attributed to the rigidity of the C-ring causing a conformational lock of the ketone moiety, exposing only the β -face to enolate attack. The authors noted that natural (–)-samaderine E could not be synthesized as none of the experimental modifications to the aldol reaction resulted in the formation of the opposite configuration at the new stereocenter. Finally, desilylation of the C-11/C-12 diol with trifluoroacetic acid furnished **30** in 71% yield. Although the divergence of the total synthesis of (–)-samaderine Y towards (–)-14-*epi*-samaderine E underlined the flexibility of Shing and Yeung's overall strategy, the lack of control of the C-14 stereocenter in the aldol reaction prevented the completion of two natural quassinoid target molecules.



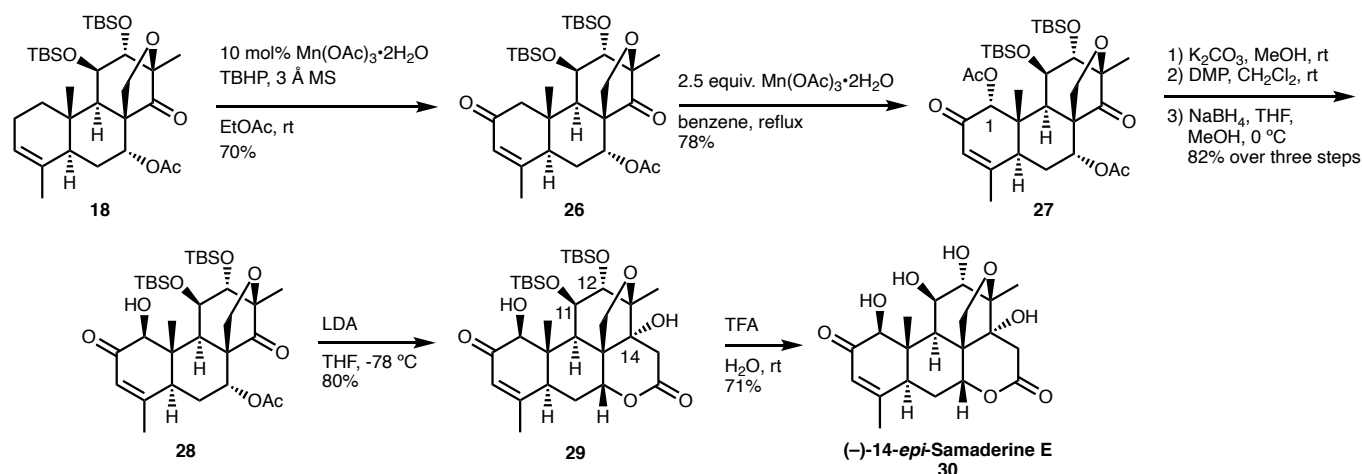
Scheme 1 Total Synthesis of (-)-Samaderine Y (**25**)

2.2. (+)-Quassin

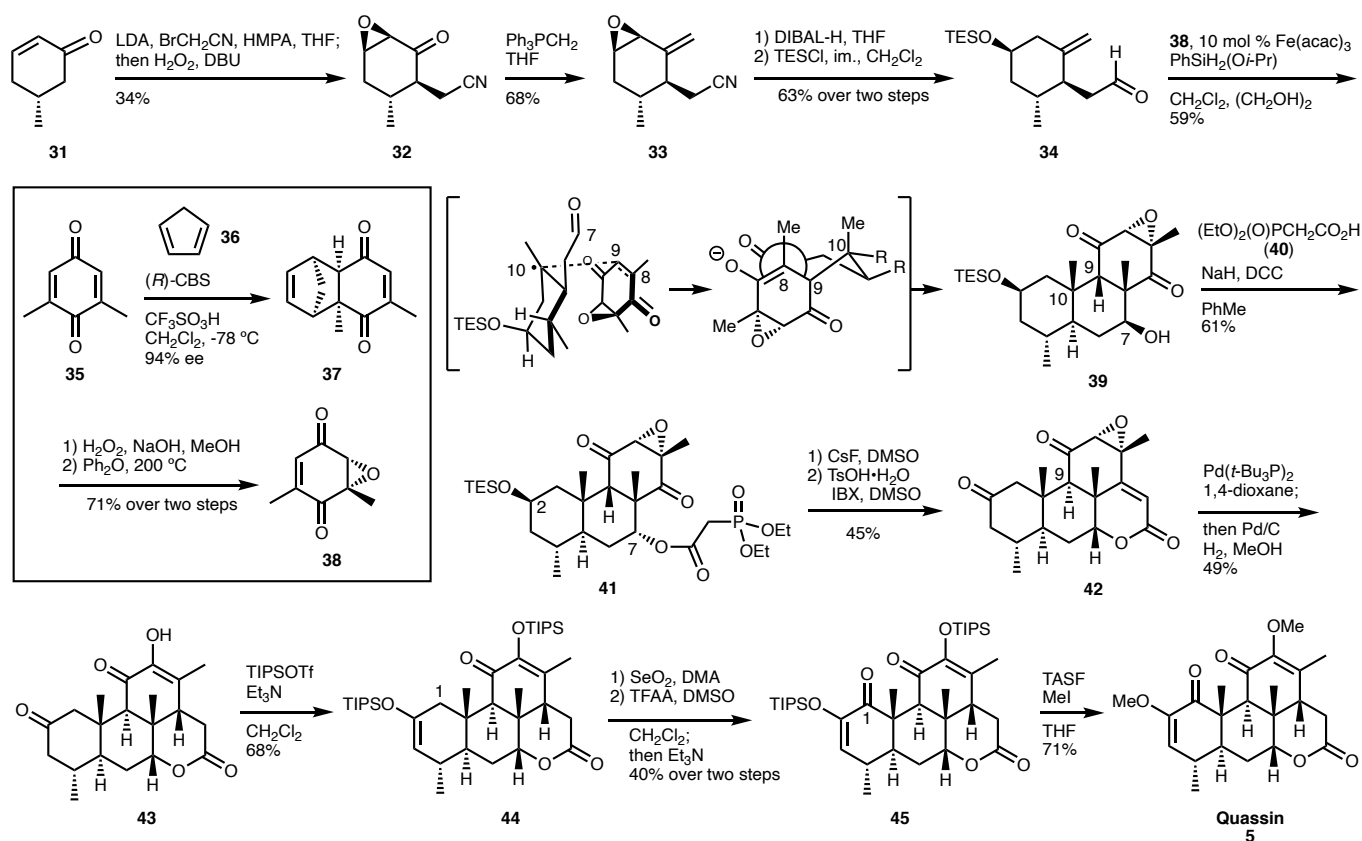
In 2022, Thomas and Pronin published a very elegant synthesis of (+)-quassin (**5**) which utilized only 14 steps from commercially available starting materials. The construction of the polycyclic core of **5** benefited from a stereoselective catalytic hydrogen atom transfer (HAT) reaction.²³

The synthesis featured the convergent assembly of two enantioenriched cyclohexane building blocks that would eventually correspond to the A- and C-rings of quassin (Scheme 3). α -Alkylation of enone **31** with LDA and bromoacetonitrile followed by epoxidation with hydrogen

peroxide delivered **32** in 34% overall yield. Wittig reaction of **32** with methylenetriphenylphosphorane afforded **33** which, upon reduction with diisobutylaluminum hydride (DIBAL-H) and subsequent silylation, led to the A-ring building block **34**. In parallel, an enantioselective Diels–Alder (DA) reaction of *p*-quinone **35** with cyclopentadiene in the presence of Corey's oxazaborolidine (*R*)-CBS catalyst gave tricyclic **37** in 94% ee in unreported yield. The DA-adduct directed the face-selectivity of the epoxidation of **37** with basic hydrogen peroxide, and cyclopentadiene was subsequently ejected with a thermal retro-Diels–Alder reaction to provide the C-ring fragment **38**.



Scheme 2 Synthesis of (-)-14-epi-Samaderine E (30) from Intermediate 18



Scheme 3 Total Synthesis of (+)-Quassin (5)

Fe(acac)₃-promoted HAT catalysis of γ,δ -unsaturated aldehyde **34** generated a tertiary radical which was trapped in a Giese addition with **38**. The resulting α -radical was then reduced to an enolate and cyclized onto the tethered aldehyde to furnish the B-ring in **39**. The Giese addition was highly diastereoselective due to the stereocontrol from the β -methyl group in **38**, although the stereocenter at C-9 needed to be

inverted later. The stereoselectivity at C-7 can be attributed to the avoidance of eclipsing interactions between the oxygen atoms of the aldehyde and incoming enolate. Similar to the C-9 stereocenter, the configuration at the C-7 position needed to be corrected at a later stage. However, the authors postulated that facile epimerization at C-7 could be accomplished through a reversible retro-aldol reaction. This was realized by treating **39** with a strong base such as sodium hydride. Subsequent trapping

of the thermodynamically favored epimer by a Steglich esterification with diethylphosphonoacetic acid and DCC generated phosphonate **41**. Treatment of **41** with CsF in DMSO led to epimerization at C-9 and closure of the D-ring through an intramolecular olefination. A mixture of silylated and deprotected C-2-alcohol products were obtained; however, this was inconsequential as oxidation with IBX in the presence of *p*-toluenesulfonic acid hydrate converted the mixture to a single polycyclic ketone, **42**, in 45% yield over the two steps. Rearrangement of the α,β -epoxy ketone in **42** into a 1,2-dicarbonyl species was accomplished through the use of a Pd(0) catalyst. Next, one-pot addition of Pd/C and H₂ hydrogenated the resulting alkene to give diosphenol **43**. TIPS-protection and silyl enol ether formation followed by allylic oxidation at C-1 with SeO₂ and a successive Swern reaction afforded **45**. Finally, a global deprotection and methylation of the two hydroxyl groups provided the target natural product in 71% combined yield. The overall yield in this sequence based on intermediates **34** and **38** was 1.5%.

The concatenation of diastereoselective bond formations that resulted from the initial HAT-catalyzed cyclization thus resulted in an impressively concise synthesis of quassin. Several stereochemical inversions were necessary but were only mildly detrimental to the overall efficiency of this sequence as they occurred concomitantly with the further evolution of the molecular complexity.

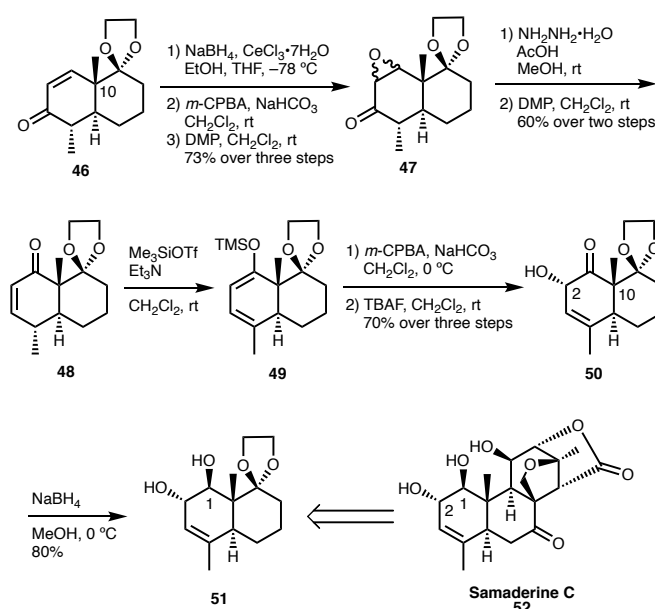
One drawback of this strategy is that it would be difficult to adapt it to the synthesis of unnatural analogs or other quassinoids besides quassin (**5**). The approach is highly dependent on the success of the initial HAT reaction and the ability to generate diverse structures rests on the scope of cyclization precursors. For example, to construct an oxide or hemiketal bridge between C-8 and C-11 or C-13, a motif that is common in many C₂₀ quassinoids (see **4** and **7**, Figure 1), **38** must possess a synthetic handle in lieu of a methyl group on the double bond. Another example would be the synthesis of quassinoids oxidized at C-6. This would require a functional group to be installed alpha to the aldehyde in **34** or additional site-selective oxidations after cyclization. Constructing appropriately functionalized precursors that could react stereo- and regioselectively might be a daunting challenge and require a significant number of extra steps. Regardless, this concise synthesis of **5** sets a new benchmark in the total synthesis of this class of natural products.

3. Synthesis of Advanced Intermediates of Quassinoid Natural Products

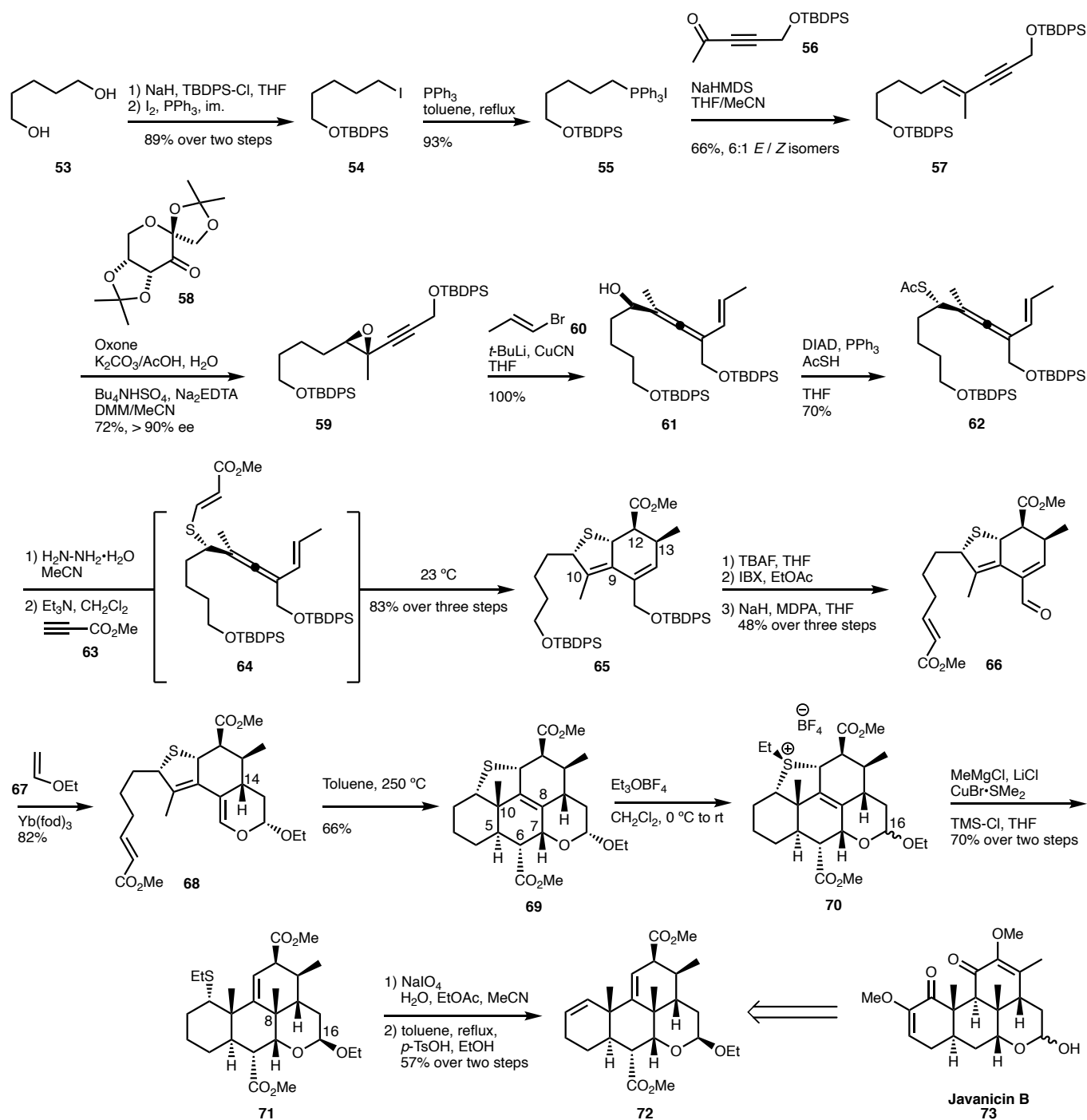
3.1. Ring A of Samaderine C

In 2013, the O'Brien group developed a 12-step sequence to access the A-ring of samaderine C (**52**) including the *trans*-1,2-diol functionality (Scheme 4).²⁴ The stereoselective synthesis of decalin **51** was completed in 7.8% overall yield.

Direct epoxidation of cyclic enone **46**²⁵ failed due to steric hindrance from the axial methyl group; therefore, a three-step reduction-epoxidation-oxidation sequence was performed. Fortunately, the sequence could be telescoped to provide **47** as an inconsequential mixture of diastereomers in 73% yield. Wharton rearrangement of **47** with hydrazine hydrate and acetic acid followed by DMP oxidation gave the 1,3-carbonyl transposition product **48**. Enolization of **48** with TMSOTf and Et₃N provided diene **49** which underwent *in situ* Rubottom oxidation to give **50** as a single diastereomer in 70% yield over three steps. The configuration of the C-2 hydroxyl group indicated that epoxidation occurred on the α -face, opposite to the neighboring β -methyl group. Reduction of **50** with sodium borohydride was also subject to a high degree of stereocontrol from the C-10 methyl group and provided *trans*-diol **51** as the major diastereomer in 80% yield. Unfortunately, the synthesis was quite lengthy, lacked new C,C-bond formations, and involved a significant number of oxidation/reduction steps. However, conversion of silyl-substituted diene **49** to diol **51** through a Rubottom oxidation and subsequent diastereoselective reduction offers a creative way to construct the *trans*-1,2-diol functionality in samaderine C (**52**).



Scheme 4 Synthesis of the Ring A Moiety of Samaderine C (**52**)



Scheme 5 Synthesis of an Advanced Javanicin B Intermediate via a Triple Diene-Transmissive Diels–Alder Approach

3.2. Polycyclic Framework of Javanicin B

The Spino group utilized a diene-transmissive Diels–Alder approach to build the framework of various tetracyclic quassinoids.^{26–29} Their strategy succumbed to multiple evolutions as countless challenges appeared along the synthetic path. The most recent reported application of this approach was towards the synthesis of javanicin B (**73**, Scheme 5).²⁹ Although the total synthesis of the natural product was not entirely realized, an advanced intermediate **72** containing the tetracyclic core and several sterically encumbered stereocenters was generated in 18 steps.

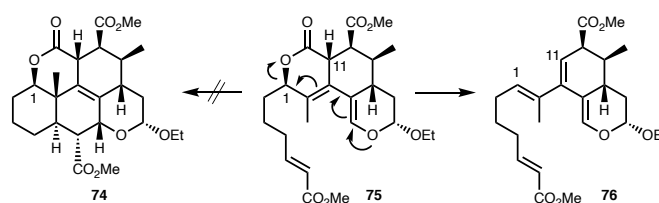
The Spino synthesis was dependent on the success of three DA cycloadditions. The precursor for the initial cycloaddition was prepared efficiently starting from 1,5-pentandiol (**53**, Scheme 5). Selective protection of one hydroxy group of **53** followed by an Appel reaction in the presence of imidazole (im.) generated alkyl iodide **54**. Conversion to the corresponding phosphonium iodide **55** and Wittig condensation with ketone **56** gave enyne **57** in a 6:1 ratio of *E*- to *Z*-isomers. Shi epoxidation gave enantiopure epoxyalkyne **59** which underwent epoxide ring opening upon treatment with a vinylcuprate reagent. Mitsunobu reaction of

allene **61** with thioacetic acid introduced a sulfur heteroatom that played a vital role in the success of the third DA cycloaddition. For the staging of the first DA, deacetylation of **62** was followed by addition to methyl propiolate to afford intermediate **64**, which underwent a rapid intramolecular [4+2] cycloaddition to **65** upon warming to room temperature. It was critical that this first DA was performed intramolecularly to get the correct geometry of the C-9/C-10 double bond. Previous attempts had shown that an intermolecular delivery of the dienophile resulted in a preferential attack on the least-hindered face of the diene to give the undesired product.³⁰ The configuration generated at the C-12 and C-13 positions was inconsequential as javanicin B (**73**) possessed a double bond between those two carbon atoms. Desilylation of the cycloadduct followed by oxidation and a chemoselective Horner-Wadsworth-Emmons reaction with methyl 2-(dimethoxyphosphoryl)acetate (MDPA) gave **66** in 48% yield over three steps. A second DA cyclization furnished **68** in 82% yield with the dienophile approaching from the *endo*-position and the more accessible face of the diene to give the desired C-14 configuration.

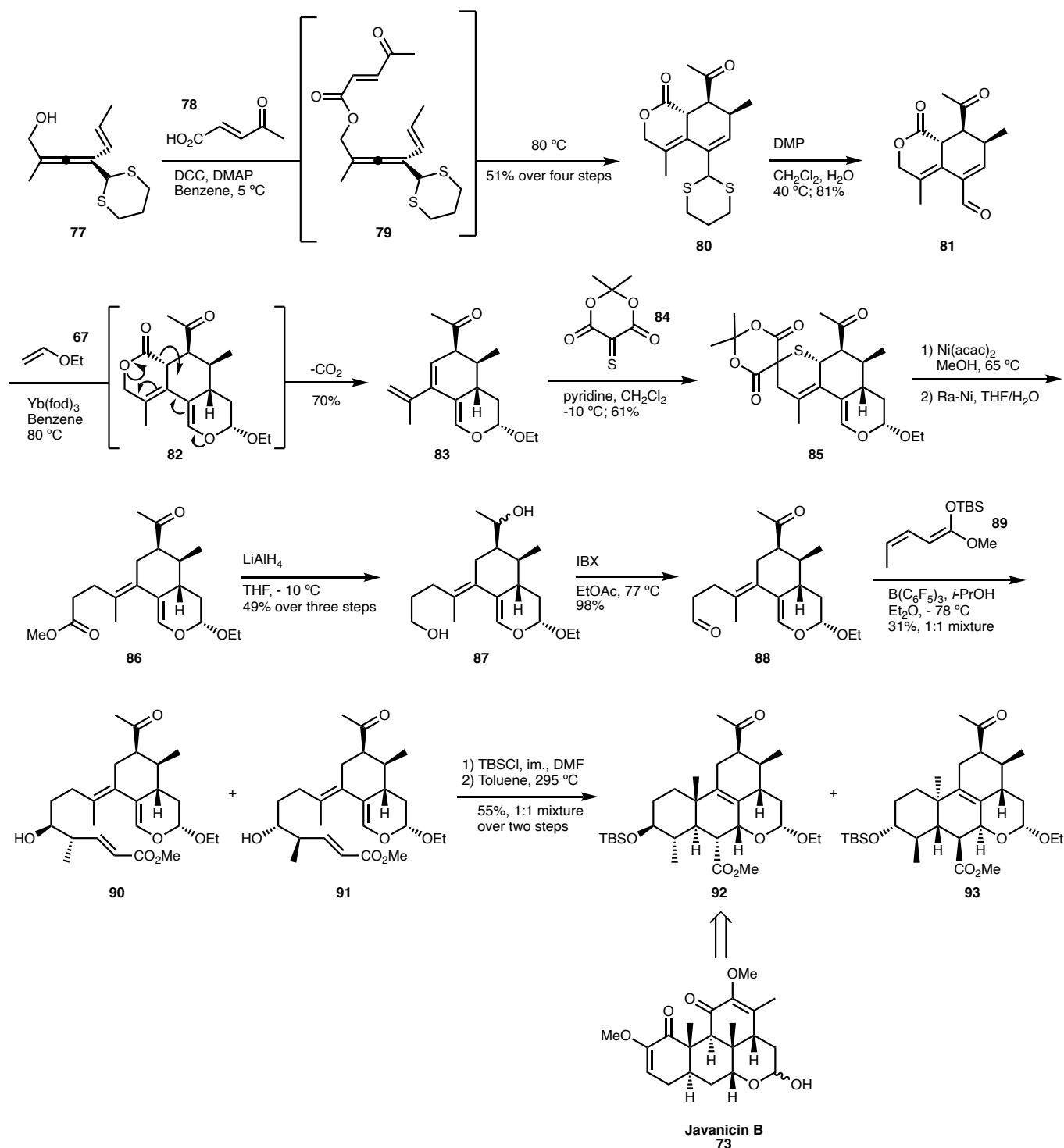
The final DA reaction proved to be the most challenging due to a competing decomposition pathway that occurred in the presence of other heteroatoms besides sulfur at C-1 (Scheme 6). For example, if the C-1/C-11 linker was a lactone such as **75**, cyclization conditions would result in decarboxylation to give **76** rather than the desired product **74**. Fortunately, the use of a sulfide bridge in **68** (Scheme 5) allowed the formation of the desired cycloadduct, presumably due to the lack of side reactions that can occur should the diene reversibly isomerize and unveil a thiolate. In one step, this DA reaction engendered the AB rings of javanicin B and established three stereocenters, including an all-carbon quaternary center, that are present in the natural product. Additionally, the resulting double bond between C-8 and C-9 provided a functional handle for the stereoselective installation of the hindered methyl group at C-8, even though the double bond's endocyclic position made this transformation quite challenging.

Success in installing the C-8 methyl group was achieved upon first converting **69** into ethylsulfonium salt **70** and then treating it with a methyl cuprate reagent. Interestingly, the authors observed epimerization at the acetal carbon C-16 during the initial sulfonium salt formation, for which they noted that the ratio of epimers could be controlled by changing the temperature. Regardless, they found that allowing the reaction to proceed at room temperature and C-16 to epimerize predominately to the β -position resulted in a cleaner subsequent reaction with methyl cuprate. The last objective to be completed was the elimination of the remaining ethyl sulfide which was accomplished by oxidation of **71** to the corresponding sulfoxide and heating in the presence of acid to give **72**. From this tetracyclic intermediate, only a few structural modifications remain to realize the total synthesis of javanicin B (**73**). Interestingly, every ring in this intermediate was constructed via a Diels–Alder reaction, highlighting the power of this pericyclic reaction in constructing functionalized 6-membered rings both intermolecularly and intramolecularly. The utilization of a sulfide tether for the cyclization to the A/B ring system and for installation of the C-8 methyl group after formation of the tetracyclic framework offered a clever solution to two major challenges in synthesizing quassinoids.

Impressively, in a separate report, Spino and Perreault utilized the decomposition pathway noted in Scheme 6 to generate a similar tetracyclic intermediate that potentially could be used for javanicin B and related quassinoids (Scheme 7).²⁸ Condensation of racemic allenyl alcohol **77** with carboxylic acid **78** generated the ester-linked intermediate **79**, which underwent an intramolecular cycloaddition upon heating to 80 °C. Lactone **80** was liable to undergo fragmentation at elevated temperatures by elimination of the allylic carbon-oxygen bond. However, this decarboxylation only occurred after conversion of the dithiane to the dihydropyran **82**. This was accomplished by oxidation of **80** with DMP to form aldehyde **81** in 81% yield. Hetero Diels–Alder reaction of **81** with ethyl vinyl ether generated the transient **82** which extruded CO₂ to form diene **83**. A DA reaction of in situ generated thione **84** with **83** was then used to introduce a masked carbon segment of ring A of the picrasane skeleton. Methanolysis and decarboxylation of **85** had to be performed with Ni(acac)₂ since standard acidic conditions resulted in decomposition. Reduction with LiAlH₄ converted **86** to the corresponding diol **87**. Double oxidation of **87** with IBX generated ketoaldehyde **88**, and a vinylogous Mukiyama aldol reaction between racemic **88** and achiral **89** generated a 1:1 mixture of diastereomers, **90** and **91**, in low yield. Of note, the reaction was reported to be completely γ - and *syn*-selective. The mixture of diastereomers was then protected with TBS-Cl and subjected to another IMDA reaction to generate **92** and **93** which could be separated chromatographically. While both compounds possess the picrasane skeleton and feature synthetic handles for future structural modifications, only tetracycle **92** contains the correct relative stereochemistry for javanicin B (**73**).



Scheme 6 Competing Decomposition Pathway for Spino's Third Diels–Alder Cycloaddition



Scheme 7 Synthesis of the Tetracyclic Framework of Javanicin B via a Quadruple Diene-Transmissive Diels-Alder Approach

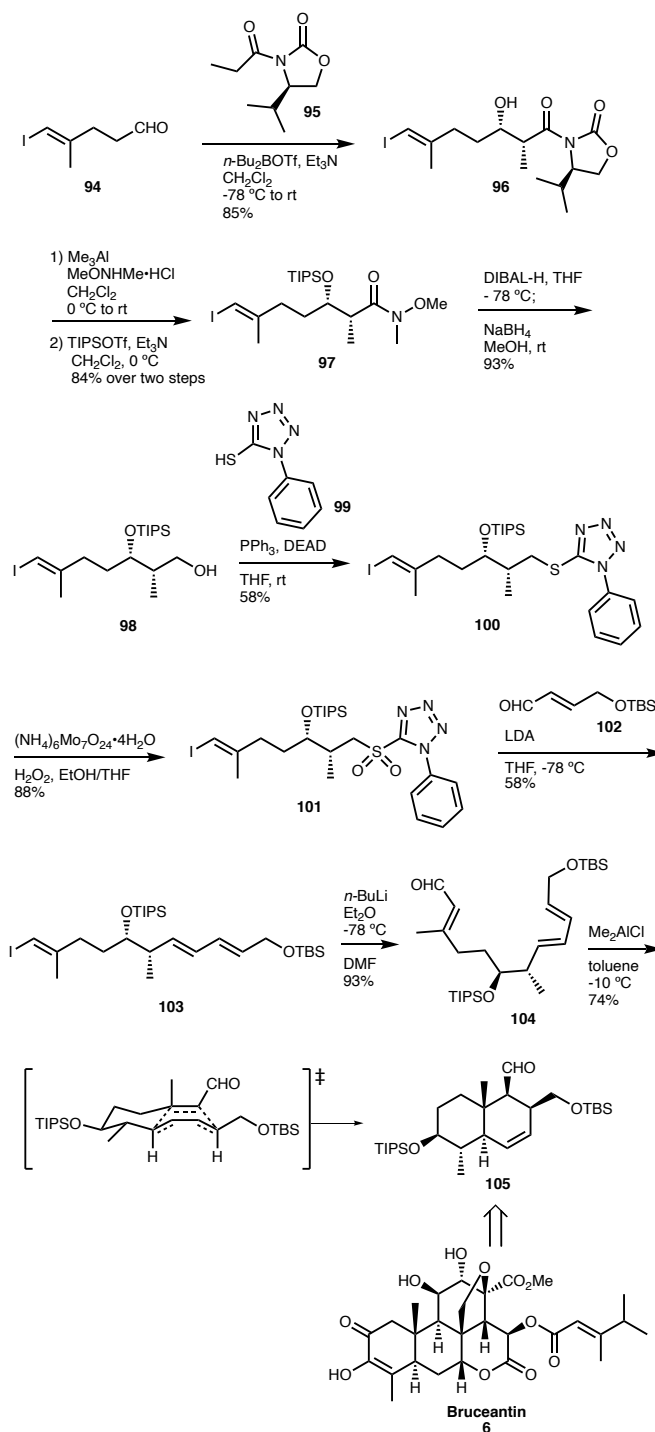
Unfortunately, because **92** does not contain the sulfide linker, introduction of the C-8 stereocenter would require a strategy that is different from the aforementioned ethylsulfonium salt approach. Once again, the Diels-Alder reaction demonstrated its potential in quassinoid synthesis both as an intermolecular and an intramolecular variant; the cyclization of **90/91** engendered two new rings and four new stereogenic carbons including an all-carbon quaternary center. Furthermore, the vinylogous aldol reaction

between **88** and **89** was particularly useful for introducing new stereocenters and provided the carbon backbone for rings A and B. An asymmetric version of this reaction on enantiopure **88** would significantly improve this synthesis, and indeed the authors noted that they were pursuing this strategy.

3.3 Rings A and B of Bruceantin via Intramolecular Cyclization

From 2015 to 2018, Nakada published two efficient approaches toward bruceantin's ring system. In the first route, a synthesis of bruceantin's AB ring system was accomplished with a stereoselective DA reaction (Scheme 8).³¹ The cycloaddition precursor was obtained by an Evans aldol reaction of aldehyde **94** with imide **95** to generate **96** in 85% yield. The aldol product **96** was then converted to the hydroxamide and protected with TIPSOTf to give **97**. Reduction with DIBAL-H and NaBH₄ followed by Mitsunobu reaction of the primary alcohol **98** with **99** afforded sulfide **100**. Oxidation of the sulfide to the corresponding sulfone with H₂O₂ and a molybdenum catalyst gave fragment **101** that was subjected to Julia–Kociensky coupling with aldehyde **102** to result in a 58% yield of *E,E*-diene **103**. The corresponding *Z*-isomer could be separated from the reaction mixture and was isolated in 9% yield. Halogen-metal exchange of **103** with *n*-BuLi and formylation with DMF afforded aldehyde **104**, which was correctly situated for an IMDA reaction. Obtaining a productive conversion from the IMDA process was challenging as most thermal and Lewis acid conditions resulted in decomposition products. The use of Me₂AlCl gave adequate yields but also produced a mixture of diastereomers at room temperature and 0 °C. At -10 °C, however, treatment of **104** with Me₂AlCl in two batches over the course of 24 h provided decalin **105** in 74% yield as a single diastereomer. Accordingly, two rings and four stereocenters of bruceantin (**6**) were generated in the DA reaction. Additionally, intermediate **105** possesses several substituents that could be utilized for completing the target molecule. For example, its aldehyde moiety would be particularly useful for constructing the C-ring and the TIPS protected hydroxy group could direct future oxidations of the A-ring. The TBS-protected primary alcohol would be well suited for constructing the THF bridge through an S_N2 process.

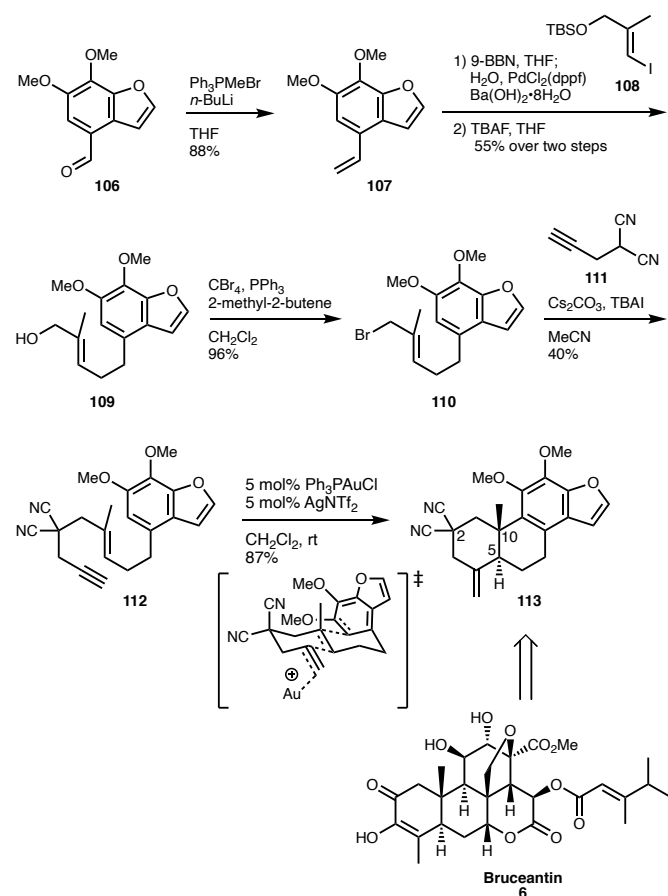
In Nakada's second approach, bruceantin's ring system was constructed through a gold-catalyzed intramolecular ene-yne cyclization of a precursor containing substituents that could later be converted into bruceantin's dense oxygen array. In addition to acting as synthetic handles, these substituents would accelerate cyclization through the Thorpe-Ingold effect.³²



Scheme 8 Synthesis of the AB Moiety of Bruceantin (**6**) via a Diels–Alder Reaction

Assembly of the enyne cyclization precursor began with the known aldehyde **106**³³ (Scheme 9). A Wittig reaction converted the aldehyde moiety in **106** into the vinyl group in **107**. Suzuki coupling with **108** and subsequent desilylation with TBAF afforded allylic alcohol **109** in 55% yield over two steps. An Appel reaction then generated bromide **110** in 96% yield, and a Finkelstein conversion to the iodide and S_N2 attack by the anion of **111** afforded the penultimate intermediate in this sequence. Finally, **112** was cyclized

in the presence of a gold catalyst to attach the AB ring skeleton of bruceantin to the benzofuran. Of note, other geminal substituents at C-2 such as methyl esters or sulfonyl groups did not lead to successful cyclization. Likewise, if C-2 was an unsubstituted methylene group the corresponding enyne was unable to produce any desired product. These results were attributed to a 1,3-diaxial interaction that occurred in the transition state between a geminal substituent at C-2 and the methyl group at C-10. The smaller size of the cyanide moiety attenuated the steric interaction and allowed for cyclization to occur. However, a lack of substituents at C-2 resulted in an unsuccessful cyclization, indicating that the Thorpe-Ingold effect was necessary for cyclization to proceed. Overall, the bruceantin ring system was generated efficiently, and an enantioselective variant of this synthesis would be very attractive for completion of the natural product.



Scheme 9 Synthesis of the Bruceantin (**6**) Framework via a Gold-Catalyzed Ene-yne Intramolecular Cyclization

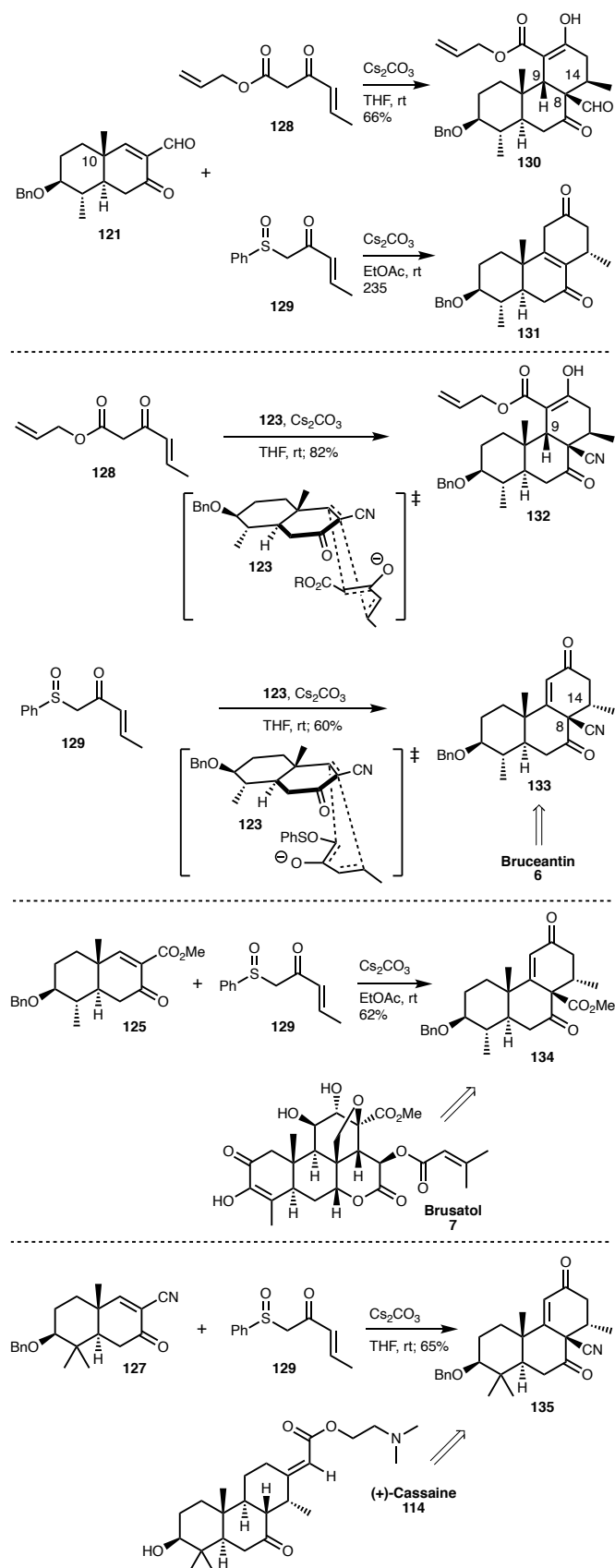
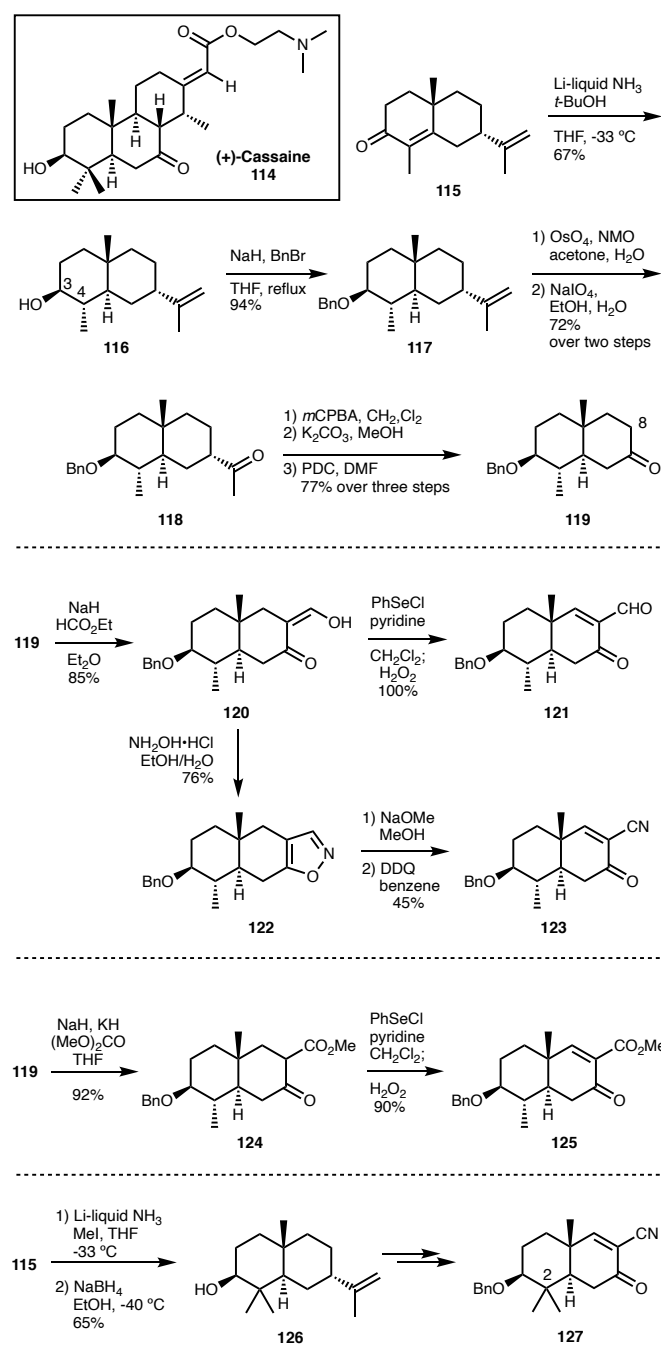
3.4. ABC Ring System of Picasane through Anionic Polycyclization of Enones with Nazarov Reagents

Deslongchamps and co-workers reported a full account of their strategy to various quassinoids and triterpenoids that utilized the reaction of α -functionalized enones with Nazarov esters and sulfoxides to prepare a library of tricyclic enones. Additionally, one intermediate was suitable for the total synthesis of (+)-cassaine (**114**, Scheme 10).^{34–36}

The synthesis of the α -functionalized enone precursor for cyclization began from known enone **115**, which is derived from natural carvone.³⁷ Enone **115** was reduced to alcohol **116**, bearing the *trans*-stereochemistry between C-3 and C-4. Benzoylation of the hydroxyl group with benzyl bromide and NaH generated benzyl ether **117** in 94% yield. Cleavage of the isopropenyl group in **117** was accomplished through dihydroxylation with OsO₄ and subsequent treatment with NaIO₄. Bayer–Villiger oxidation of the resultant ketone followed by deacetylation and another oxidation with PDC gave **119** in 77% yield over three steps. The synthesis then diverged from ketone **119** with the goal to install an array of functional groups at C-8.

Treatment of **119** with sodium hydride and ethyl formate generated α -formyl ketone **120** which was converted to α -formyl enone **121** by phenylselenation followed by oxidative elimination. Additionally, condensation of **120** with hydroxylamine hydrochloride gave isoxazole **122** as the major regioisomer. Isoxazole **122** was opened to the corresponding α -cyano ketone with sodium methoxide, and subsequent oxidation with DDQ gave enone **123**. Ketone **119** could also be converted to α -carbomethoxy ketone **124** upon treatment with sodium hydride and dimethyl carbonate. This intermediate was then converted to enone **125** according to the previous phenylselenation/oxidative elimination sequence. Functionalized enone precursors possessing a geminal dimethyl group at C-2 could be synthesized following the same sequence but with a slight modification in the initial step. Reductive methylation of **115** generated dimethyl alcohol **126** which was subjected to the same sequence as **116** to generate the corresponding α -functionalized enones such as **127**. Compounds **121**, **123**, **125**, and **127** represent useful intermediates in their own right as they contain two rings, multiple stereocenters, and several functional groups. The generation of a structurally diverse collection of compounds from a single intermediate demonstrated the synthetic flexibility of this sequence.

The cyclization of activated cyclic enones with Nazarov reagents **128** and **129** was then performed to construct the C-ring of the picrasane skeleton (Scheme 11). Cyclization of α -formyl enone **121** with ester **128** in the presence of Cs₂CO₃ at room temperature gave the expected tricycle **130** in 66% yield. However, reaction of **121** with sulfoxide **129** resulted in only 23% of tricycle **131** which arose from elimination of the sulfoxide and formyl groups. Similarly, cyano enone **123** reacted as expected with ester **128** to give the tricycle **132** from an *endo*-transition state. Cyclization of **123** with sulfoxide **129** also provided the expected tricycle; and after chromatography on SiO₂, the sulfoxide was eliminated to give **133**. Reaction of carbomethoxy enone **125** and sulfoxide **129** afforded **134** which is analogous to enone **133** in terms of stereochemistry. Finally, the C-2 geminal dimethylated α -cyano enone **127** reacted with sulfoxide **129** to give the expected tricycle **135**, which was carried forward toward the total synthesis of (+)-cassaine (**114**). These reactions proved to be highly efficient for increasing molecular complexity as most examples formed the C-ring in good to high yields. Reactions with **128** led to highly oxygenated final products and reduced the need for future site-selective oxidations. Finally, all reported cyclizations were stereoselective and established up to three new stereocenters.



The configuration at the C-9 position of **130** and **132** was controlled by the axial C-10 methyl group, which forced **128** and **129** to approach from the α -face of the reacting enone. Interestingly, orientation at the C-14 stereocenter was dependent on whether ester **128** or sulfoxide **129** were used for the cyclization and the two reagents are believed to react by two different mechanisms. In instances where the ester Nazarov reagent was used, the final product possessed a C-8/C-14 *cis*-relationship due to a formal double conjugate addition reaction. In contrast, use of the sulfoxide Nazarov reagent afforded a C-8/C-14 *trans*-relationship as a result of an *endo* Diels–Alder reaction.

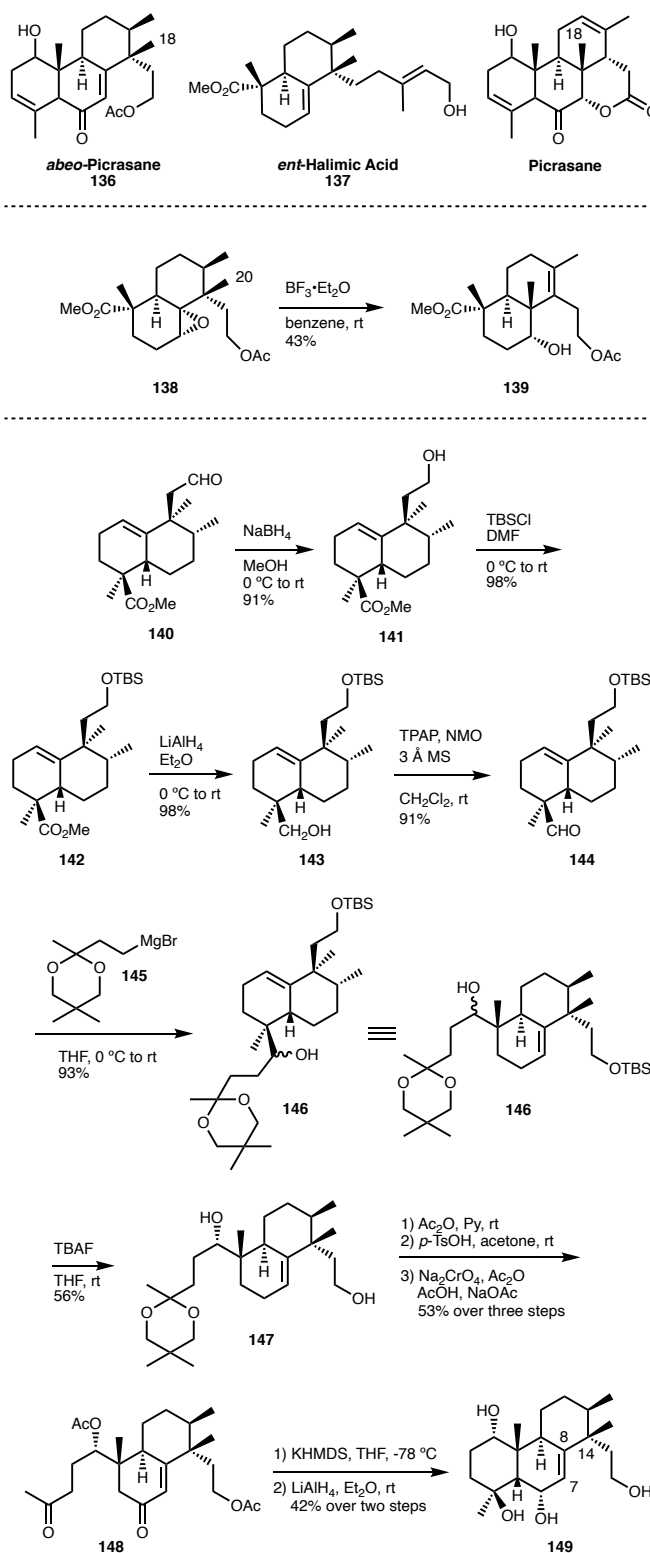
Notably, **133** and **134** contain several stereocenters present in bruceantin (**6**), brusatol (**7**), and related quassinoids. The correct installation of the C-8 stereocenter is especially impressive as it is known to be quite challenging to establish. Additionally, the enone, keto, carbomethoxy, and cyano moieties allow for facile conversions and modifications of the C- and D-rings. Therefore, tricycles **133**, **134** and **135** could serve as useful intermediates for the asymmetric synthesis of these quassinoids.

3.5. Picrasane Skeleton from a Methyl Rearrangement Reaction

Marcos and associates reported the synthesis of an *abeo*-picrasane intermediate which was demonstrated to undergo an interesting methyl rearrangement to access the ABC ring system of picrasane and concomitantly install the C-8 stereocenter (Scheme 12).³⁸ The *abeo*-picrasane intermediate was synthesized from known decalin **140**,³⁹ which is derived in seven steps from the readily available *ent*-halimic acid (**137**).

Prior to synthesizing the desired intermediate, Marcos tested their strategy on a model substrate, converting an *ent*-halimane into an *ent*-labdane skeleton. Interestingly, this process represents an inverse biosynthetic pathway. Treatment of **138** with $\text{BF}_3 \cdot \text{OEt}_2$ resulted in Lewis acid coordination to the epoxide and subsequent C-20 methyl migration with epoxide ring opening. The ensuing E_1 elimination furnished the *ent*-labdane skeleton in **139** in a modest 43% yield. Considering the model reaction a success, the authors began the assembly of a tricyclic *abeo*-picrasane intermediate to effect this rearrangement.

Reduction of the aldehyde in **140** with sodium borohydride gave primary alcohol **141**. Silylation of the free hydroxy group and reduction of the methyl ester followed by Ley oxidation afforded aldehyde **144**. Alkylation of **144** with Grignard reagent **145** gave **146** as a mixture of diastereomers. After desilylation with TBAF, the mixture of diastereomers could be separated by chromatography. Diastereomer **147** was acetylated with Ac_2O in pyridine and removal of the 1,3-dioxane protecting group under acidic conditions gave, after allylic oxidation with $\text{Na}_2\text{Cr}_2\text{O}_7$, intermediate **148**. Compound **148** was subjected to an intramolecular aldol condensation to furnish the A-ring, and global reduction afforded *abeo*-picrasane **149**. The remaining steps included an electrophilic epoxidation of the C-7/C-8 double bond and a methyl rearrangement to install the C-8 methyl group of picrasane. Additionally, the tethered alcohol side chain at C-14 could be utilized to annulate the D-ring and thus complete the construction of the picrasane skeleton.



Scheme 12 Methyl Rearrangement Strategy to Access the Picrasane Skeleton from *abeo*-Picrasane

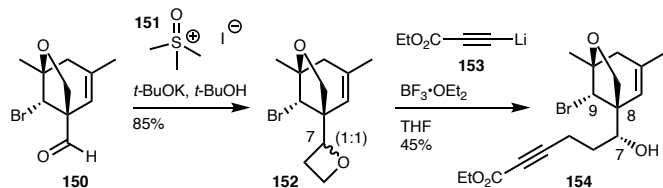
This synthesis employs a substantial number of oxidation/reduction steps and protecting group manipulations to synthesize one ring of the picrasane skeleton, reducing its overall efficiency. However, the methyl-rearrangement/epoxide opening sequence performed on **138** is very instructive as it installed a

quaternary stereocenter and positioned **139** for subsequent cyclization of the D-ring. Ideally, a substrate like **149** would be synthesized more efficiently from simpler starting materials. It should be noted that the methyl-rearrangement/epoxide opening reaction on **149** was not reported; instead, the authors stated that the reaction would be investigated in the future.

3.6. C₂₀ and C₁₉ Quassinoid Skeletons Through Radical Cyclization

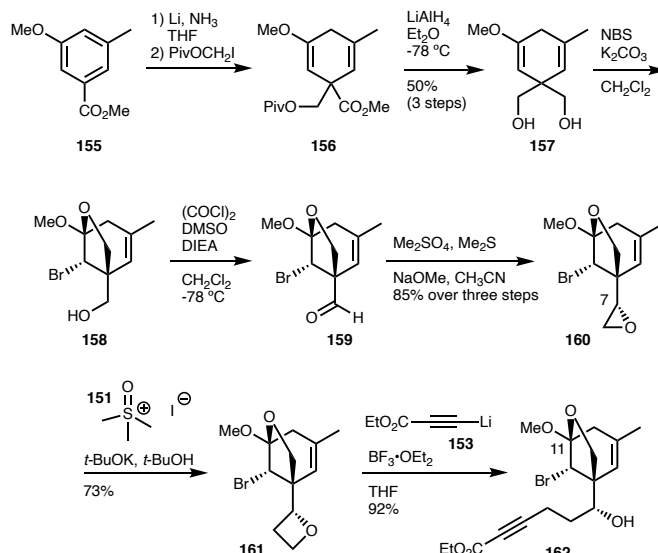
Several functionalized tricycles possessing the BCE-ring structure of C₂₀ and C₁₉ quassinoids were synthesized by Hart, Yang, Donahue and associates. These tricycles were prepared from the intramolecular radical cyclization of bromoalkynes and could serve as potential intermediates for the total synthesis of quassinoids such as 3,4-dihydro excelsin or polyandran. ^{40–42}

The six-membered B-ring of the picrasane skeleton was hypothesized to arise upon cyclization of compounds such as **154**, which bears an alkynyl side chain tethered to the C-8 position and a bromine at the C-9 position (Scheme 13). Bromoalkyne **154** was prepared in two steps from known aldehyde **150**.⁴³ Treatment of **150** with two equivalents of dimethyloxosulfonium methylide generated oxetane **152** through an epoxide intermediate. Oxetane **152** was formed as an inseparable mixture of diastereomers, but after ring-opening with the lithium anion of ethyl propiolate, **154** could be isolated as a single diastereomer.

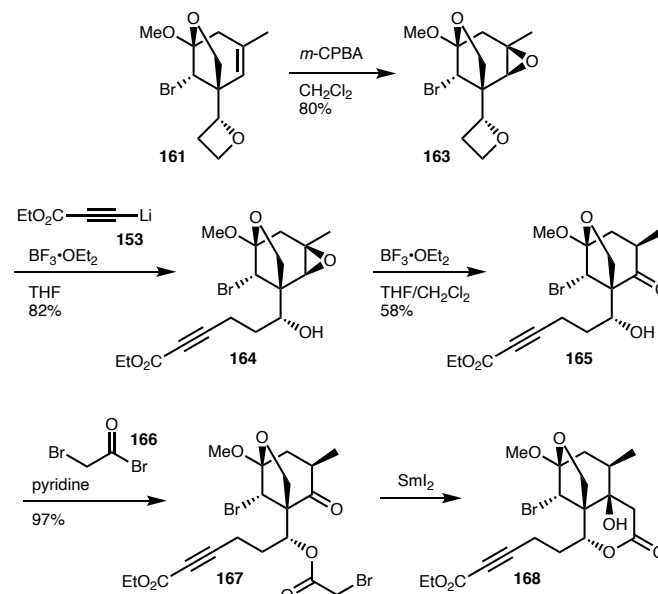


Scheme 13 Synthesis of Intermediate **154** for the Radical Cyclization Approach to C₂₀ Quassinoids

Analog **162**, containing a methoxy group at C-11 rather than a methyl group, was prepared in eight steps from benzoate **155** (Scheme 14). Birch reduction and subsequent alkylation followed by reduction with lithium aluminium hydride gave diol **157** in 50% yield over three steps. Bromoetherification of the more electron-rich alkene furnished the E-ring and correctly positioned the C-9 bromine for future radical cyclization. Swern oxidation and treatment of the resultant aldehyde **159** with dimethylsulfonium methylide gave a 2:1 mixture of epoxides which could be separated by chromatography. Pure **160** was converted to oxetane **161** upon treatment with dimethyloxosulfonium methylide and was opened with lithium ethyl propiolate to generate **162**.



Scheme 14 Synthesis of Intermediate **162** for the Radical Cyclization Approach to C₂₀ Quassinoids

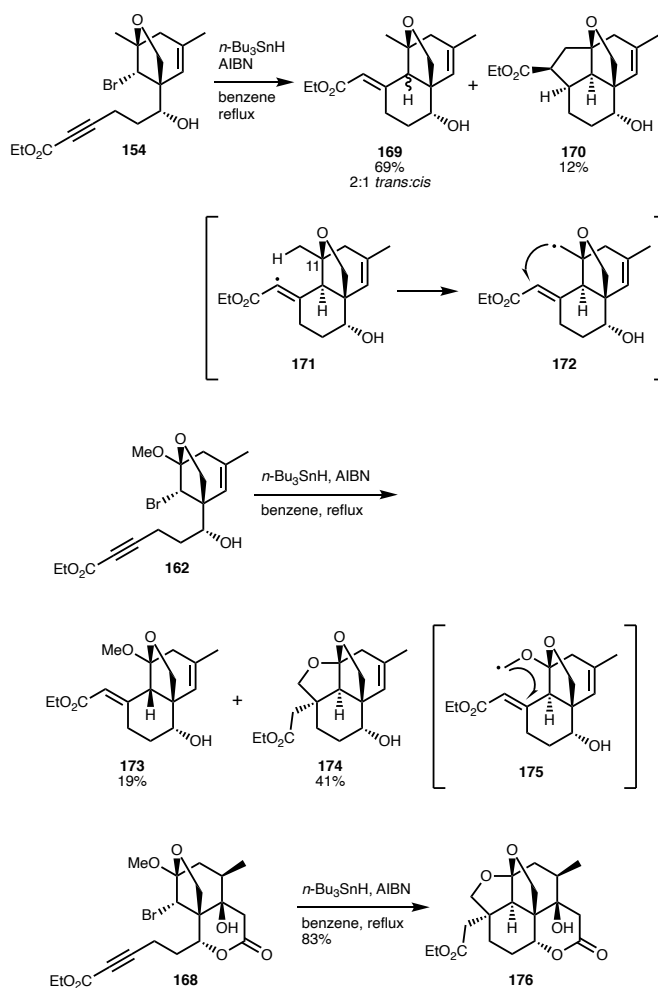


Scheme 15 Synthesis of Intermediate **168** for the Radical Cyclization Approach to C₂₀ Quassinoids

Finally, cyclization precursor **168**, which contains a fully functionalized D-ring, was prepared from the previously synthesized intermediate **161** (Scheme 15). Epoxidation of **161** with *m*-CPBA gave epoxide **163** in 80% yield, and selective oxetane opening with lithium ethyl propiolate afforded epoxy bromoalkyne **164**. Epoxide opening and 1,2-hydride shift were accomplished upon treatment with BF₃·OEt₂ in a tetrahydrofuran/methylene chloride solution. The β-hydroxy group was esterified with bromoacetyl bromide and an intramolecular Reformatsky reaction of **167** closed the D ring.

After the successful syntheses of compounds **154**, **162**, and **168**, these intermediates were tested for their ability to undergo the desired intramolecular radical cyclization (Scheme 16). Treatment of

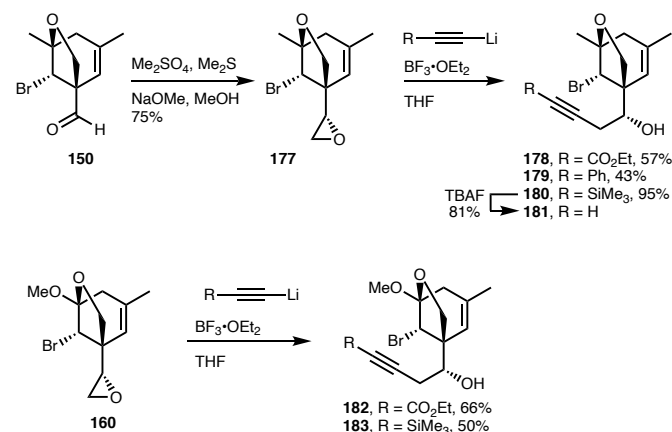
154 with $n\text{-Bu}_3\text{SnH}$ and AIBN in benzene indeed afforded the desired six-membered ring **169** in 69% yield as a 2:1 mixture of *trans*- and *cis*-fused rings. Interestingly, tetracycle **170** was generated as a minor product. Its genesis is believed to be the result of a 1,5-hydrogen atom transfer of intermediate vinyl radical **171** and the nearby C-11 methyl group of the *trans*-fused ring system. Methyl radical **172** then undergoes a 5-*endo*-cyclization to close the five-membered ring. Similarly, subjecting methoxy acetal **162** to the same conditions generated a 2:1 mixture of *trans*- and *cis*-fused ring systems in 60% combined yield. However, the *trans*-fused product performed an additional cyclization to generate tetracycle **174**, likely through a 5-*exo*-cyclization of the alkoxy radical intermediate **175**. Tricycle **168**, already bearing the D-ring lactone, cyclized exclusively to the *trans*-fused product, which also performed an additional cyclization through a transient alkoxy radical species to generate **176**. The improved *trans*-selectivity of **168** was thought to arise from the conformational constraint brought on by the D-ring. Since the synthesis of C_{20} quassinoids requires the installation of a *trans*-fused BC-ring system, the D-ring ought to be constructed prior to this radical cyclization should this strategy be pursued for total synthesis, in order to improve the stereoselectivity of the route.



Scheme 16 Radical Cyclizations of Precursors to C_{20} Quassinoids

Cyclization precursors for C_{19} quassinoids were prepared from intermediates **150** and **160** (Scheme 17). Treatment of aldehyde **150**

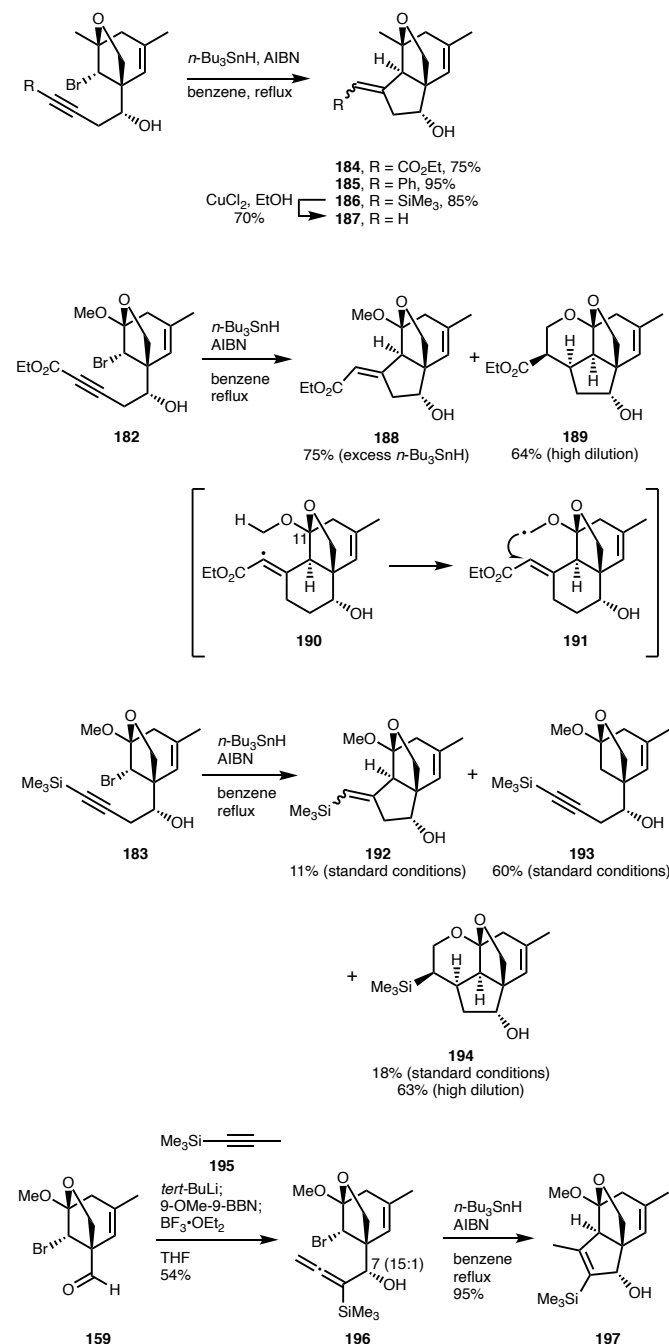
with dimethylsulfonium methylide gave epoxide **177** as a 2:1 mixture of diastereomers which could be separated by chromatography. Purified **177** was opened with a variety of acetylides to generate bromoalkynes **178-180**. Terminal alkyne **181** was generated by treatment of trimethylsilylated **180** with TBAF. Opening of previously synthesized **160** with acetylides derived from ethyl propiolate and trimethylsilylacetylene provided precursors **182** and **183**, respectively.



Scheme 17 Synthesis of Intermediates **178-183** for a Radical Cyclization Approach to C_{19} Quassinoids

Cyclization of bromoalkynes bearing a C-11 methyl group afforded products **184-186** as stereoisomers, with the notable exception of ethyl ester substituted alkyne **184**, which was formed completely *E*-selectively (Scheme 18). Deuterium labelling experiments suggested that the observed *E*-selectivity of **184** was due to the reduction of the intermediate vinyl radical occurring intramolecularly through 1,5-hydrogen atom transfer from the C-11 methyl group. Additionally, cyclization of alkynes **178-180** always produced a *trans*-fused B-ring, likely due to a greater conformational constraint in the transition state compared to their 6-membered counterparts. Cyclization of alkyne **181** gave an unsatisfactory low yield, so tricycle **187** was instead prepared by protodesilylation of **186** with CuCl_2 in ethanol, which led to a 70% yield. Interestingly, cyclization of methoxy-substituted precursors **182** and **183** gave a distribution of products depending on the reaction conditions. Treatment of **182** with an excess of tri-*n*-butyltin hydride gave the expected *trans*-fused tricycle, **188**, in 75% yield. However, slow addition of tri-*n*-butyltin hydride to diluted **182** resulted in a 1,6-hydrogen atom transfer between the methoxy group and the intermediate vinyl radical in **190** followed by a 6-*endo* cyclization of alkoxy radical **191** to give **189** after tin hydride reduction. Cyclization of **183** under standard conditions provided the desired product **192** as a mixture of stereoisomers in only 11% yield, and **194** was formed in 18% yield. In contrast, debrominated product **193** was formed predominately in 60% yield. Under high dilution conditions, **194** could be isolated in 63% yield and is believed to arise from the same pathway as **189**. As an attempt to improve the yield of the desired cyclized products such as **188** without using an excess of toxic tri-*n*-butyltin hydride, allene **196** was synthesized in one pot and with high stereoselectivity from **159**. It was postulated that upon initial radical

formation of **196**, the allylic radical would not be correctly positioned to undergo a 1,6-hydrogen atom transfer with the C-11 methoxy group. Therefore, the intermediate radical would be reduced to the desired product rather than perform a second intramolecular cyclization. Pleasingly, radical cyclization of **196** proceeded as hypothesized and tricycle **197** was synthesized in 95% yield. In addition to the high yield of *trans*-fused **197**, the high stereoselectivity of its synthesis renders it a particularly useful intermediate for C₁₉ quassinoids.



Scheme 18 Radical Cyclizations of Precursors to C₁₉ Quassinoids

The use of radical reactions such as the ones described here are particularly relevant for the synthesis of quassinoids due to radical chemistry's tolerance of Lewis basic functionalities such as ethers

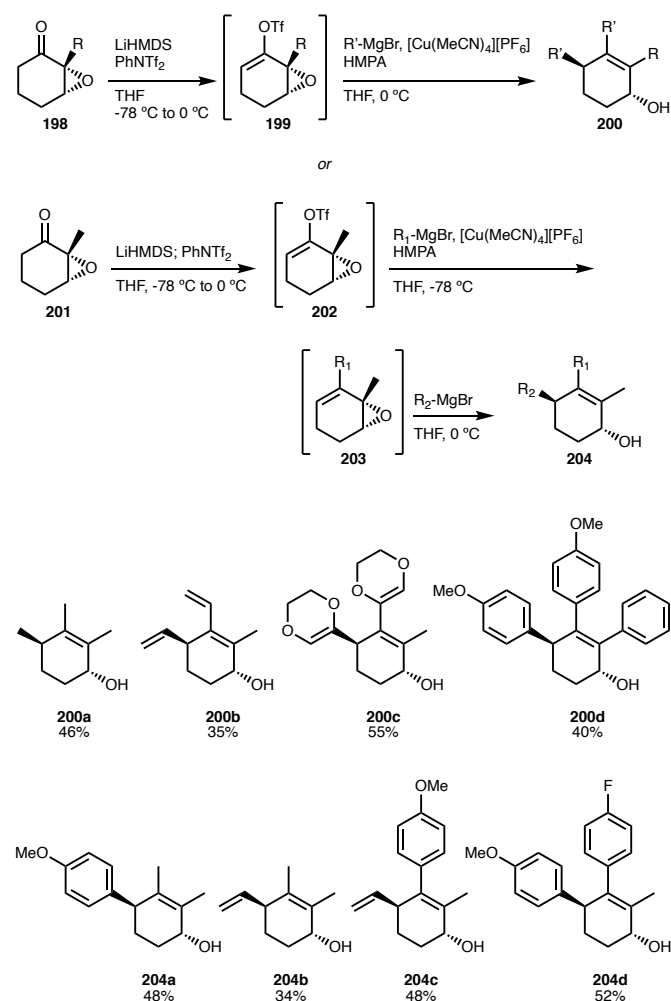
and esters, and these reactions' ability to form bonds between sterically congested sites.⁴⁴ For instance, radical cyclization of **168** proceeded in excellent yield in the presence of hydroxy and methoxy groups, a THF bridge, and a saturated cyclic lactone; in all examples, a tertiary carbon was generated adjacent to two quaternary carbon centers. However, undesired intramolecular HAT reactions and additional cyclizations should be avoided. This can be accomplished through experimental modifications such as using an excess of tri-*n*-butyltin hydride or, preferably, though judicious selection of cyclization precursors.

4. Key Methods for Accessing Quassinoid Substructures

4.1. Copper-Catalyzed Double Coupling of Vinyl Triflates with Grignard Reagents to Generate Polycyclic Compounds

An effective method for the stereoselective synthesis of polycyclic products from vinyl triflates was reported by the Maimone group in 2019. This methodology was then applied to construct the quassinoid skeleton in only three linear steps.⁴⁵ The overarching strategy was to first convert chiral epoxy ketones such as carvone epoxide **198** into vinyl triflate **199** with LiHMDS and PhNTf₂ (Scheme 19). Vinyl triflate **199** would then undergo a copper-catalyzed double addition from an alkyl Grignard reagent to give functionalized cyclohexenols. The methodology was further expanded by utilizing temperature control. By maintaining the temperature at -78 °C, the first addition of the nucleophile would be selective for cross-coupling. Subsequently, treatment with a different nucleophile and warming the reaction mixture to 0 °C would result in the S_N2'-reaction and epoxide opening. This was a particularly relevant discovery as the ability to install different nucleophiles into the same cyclohexenol substrate allows for the synthesis of a variety of quassinoid building blocks. This method could eventually be used for developing analogs of the bioactive compounds. Notably, in both approaches, allylic substitution was diastereoselective for the *anti*-isomer. Alkyl, vinyl, dioxene and aromatic Grignard reagents gave acceptable to good yields (**200a-d**). Use of the dioxene nucleophile is particularly noteworthy as four oxygens were added to the substrate **200c** in a single step in good yield and diastereoselectivity.

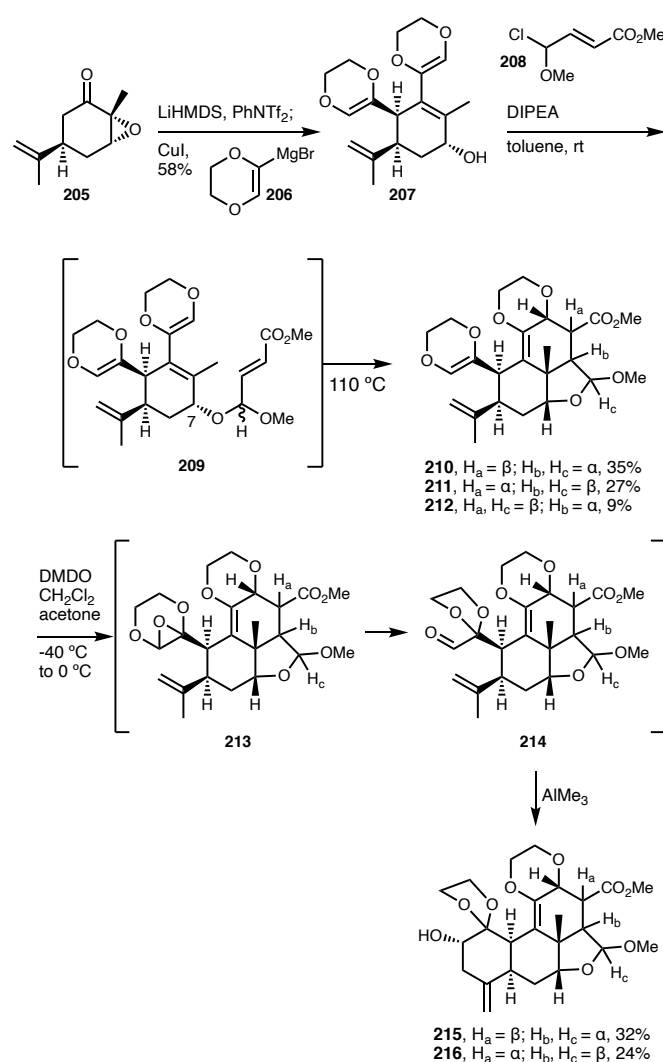
The ability to install several oxygen atoms in a single step significantly adds to the power and efficiency of this method, and further investigations to determine what other oxygen-bearing nucleophiles could be used would be an interesting extension. Additionally, both methyl and phenyl substituents on the epoxide were well tolerated (**200c-d**). These cyclohexenols could be very useful for the synthesis of the B-ring of quassinoids as the α -hydroxy group already has the correct stereochemistry for the C-7 position and the adjacent alkyl group could be leveraged for future installation of the C-8 quaternary center. Using two different nucleophiles appeared to have little effect on the isolated yields (**204a-d**) and the position of the substituents could be switched by changing the order of addition of nucleophiles and maintaining temperature control.



Scheme 19 Construction of Functionalized Cyclohexenol Building Blocks by Copper-Catalyzed Double Coupling of Vinyl Triflates

This methodology was applied to a three-step synthesis of the quassinoid skeleton (Scheme 20). The sequence began with the copper-catalyzed double addition of dioxene-based Grignard **206** to epoxy-carvone **205** to afford cyclohexenol **207** in 58% yield as a single isomer. Next, the C-7 hydroxy group was alkylated with dienophile **208** for a subsequent IMDA of **209**. Unfortunately, this alkylation was unselective and a 1:1 mixture of diastereomers was isolated which decreased the impact of the DA reaction. The configuration of the acetals directed the *endo/exo* selectivity of the IMDA and the 1:1 mixture led to three major product isomers in low to moderate yields. Ideally, future epimerization and ablation of stereocenters would eventually converge these isomers into a single product. Experimentally, carrying forward a mixture of diastereomers is less than ideal, especially if there are many steps remaining to the target molecule or the convergence of isomers. Regardless, the authors only needed one more step to complete the quassinoid architecture, carrying forward a mixture of **210** and **211**. Epoxidation of the more electron-rich alkene with DMDO resulted in spontaneous rearrangement of epoxide **213** into aldehyde **214** and treatment of the reaction mixture with AlMe_3 led to an ene-cyclization between the aldehyde and the nearby vinyl group. The cyclization was stereoselective for a single isomer at the newly formed hydroxy

group and diastereomers **215** and **216** were formed in 32% and 24% yield, respectively. Ultimately, the quassinoid core was constructed in only three steps from carvone epoxide, albeit with poor diastereoselectivity. Furthermore, there would be several challenging additional steps needed in order for this intermediate to be used for the completion of quassinoid natural products, including the installation of the C-10 methyl group and ring expansion of the D-ring lactone. Despite some of the drawbacks of the three-step synthesis, the diverse chiral building blocks this methodology can produce from readily available starting materials, and the experimental ease of controlling regioselectivity, renders it a highly effective strategy for generating quassinoid intermediates.



Scheme 20 Three Step Synthesis to Quassinoid Architecture Using Double Cross-Coupling

4.2. Synthesis of Functionalized Tricycles by Oxidative Coupling of Tethered Cyclic Ketones

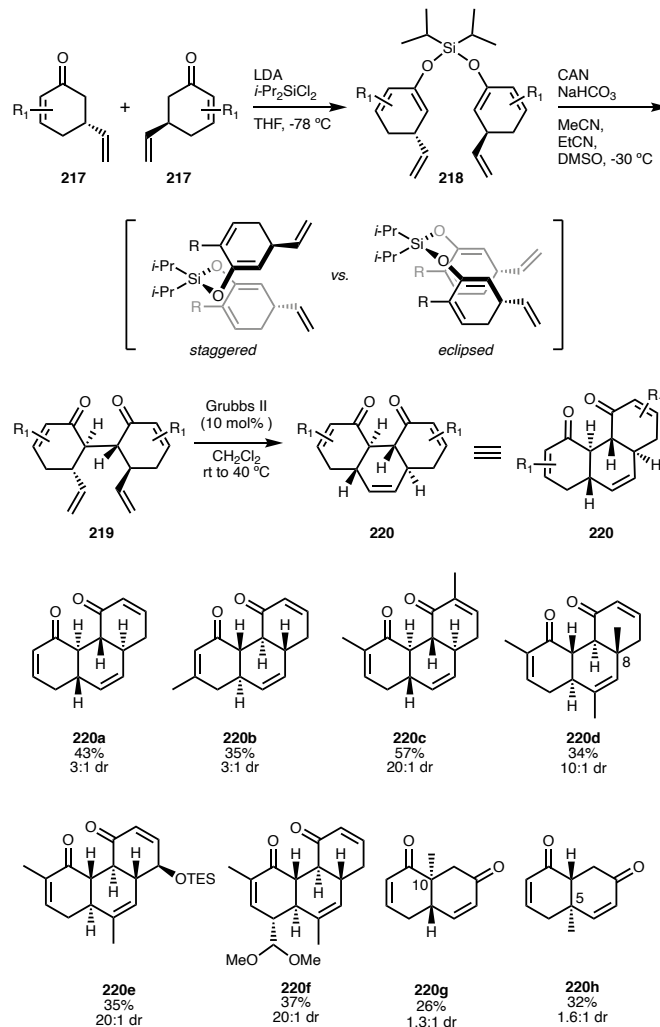
In 2018, Robinson and Thomson disclosed a “couple and close” strategy to access functionalized chiral tricycles.⁴⁶ The “couple” portion of the strategy involved the tethering of chiral cyclic enones as bis-silyl enol ethers and subsequent oxidative coupling (Scheme 21). The final “close” referred to a ring-closing metathesis of appended vinyl groups to construct 6-membered rings. Isolated products were tricyclic intermediates that possess an array of stereocenters and functional groups such as ketones and alkenes.

Cyclic vinyl enones of type **217** were deprotonated with LDA and the resulting enolate anions were treated with 0.5 equivalents of dichlorodiisopropylsilane to afford bis-silyl enol ethers **218**. Two different cyclic enones could be utilized and only the order of addition had to be adjusted: sequential addition of each lithium enolate to one equivalent of dichlorodiisopropylsilane. Fortunately, the second addition of lithium enolate into the silane was significantly slower than the initial addition, so product distribution could be easily controlled. Oxidative coupling of **218** was accomplished upon treatment with CAN to give the *trans*-isomer **219** as the major product. This stereochemical outcome was the result of the staggered conformation of the bis-silyl enol ether, avoiding steric interactions between the two β -vinyl groups and ring-to-ring eclipsing interactions. Thus, formation of the new carbon-carbon bond occurred opposite to the β -vinyl groups. Cyclization of diketone **219** with Grubbs 2nd generation catalyst gave tricycle **220** as the final product.

Reported yields for the three-step sequence fell within a range of 26–57%. Diastereoselectivity was calculated based on the oxidative coupling step and was highly dependent on substituent effects. It was poor if starting enones had no substituent (**220a**) or a C-3 substituent (**220b**). However, a C-2-substituent significantly increased diastereoselectivity (**220c-f**). This is likely due to the increased steric hindrance of the eclipsed conformation which therefore makes it even less favorable. Products containing quaternary carbons were obtained in significantly lower yields and diastereoselectivities (**220g, h**). Enones **220g** and **220h** were prepared using methyl vinyl ketone and enone **217**. No examples of tricycles possessing a quaternary center at C-10 were presented, likely due to the steric hindrance impeding the oxidative coupling of two cyclic enones. In instances where poor diastereoselectivity occurred, the authors demonstrated that the products could have their configurations adjusted in subsequent steps, although this approach distracts from the overall efficiency of the strategy.

If the cyclic enones could be densely functionalized with oxygen atoms and side chains, then this 3-step sequence would offer a convergent method for constructing the ABC-ring system of quassinoids, albeit that quaternary carbons may have to be installed in a different fashion. The biggest drawback is the poor diastereoselectivity in reactions with enones lacking a C-2 substituent. However, if a synthetic handle is installed at this position for further utilization at a later stage, this issue can be

attenuated. Another possible solution would be to install a removable “directing” group that would improve diastereoselectivity during the reaction and could then be cleaved. This strategy would be much more efficient and practical than trying to correct undesired configurations through stepwise modifications after cyclization.

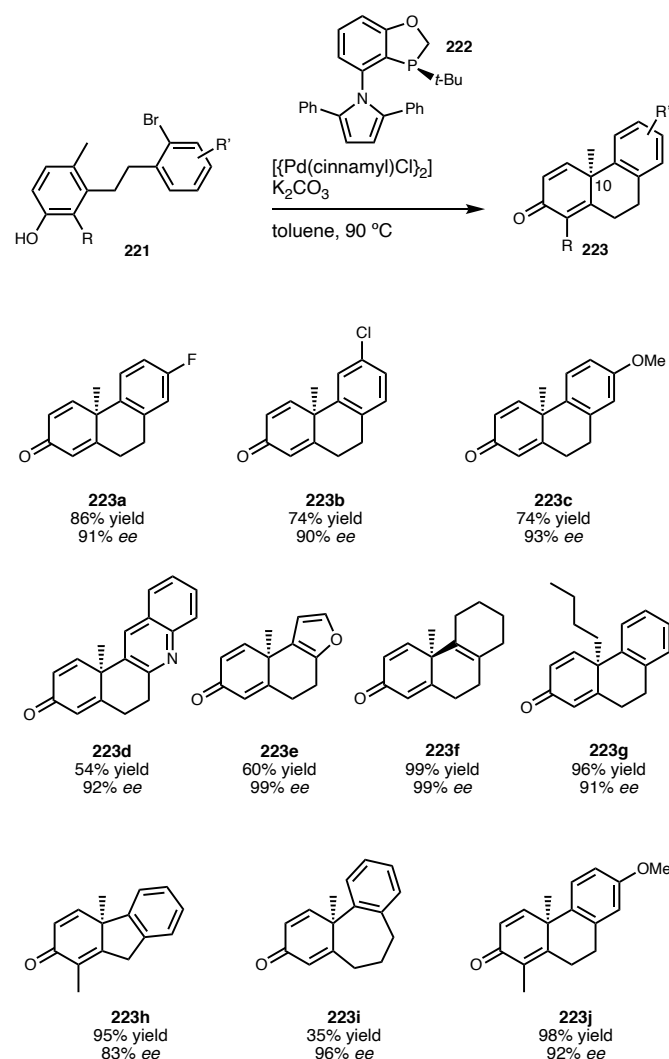


Scheme 21 Oxidative Coupling of Bis-Silyl Enol Ethers to Generate Functionalized Decalins

4.3. Construction of Polycyclic Compounds with All-Carbon Quaternary Centers through Palladium-Catalyzed Dearomative Cyclization

The Tang group devised a method for constructing a series of chiral tricycles that could be applied to the synthesis of terpenes, steroids, and quassinoids (Scheme 22).⁴⁷ In this system, bromine-substituted phenols like **221** underwent an asymmetric dearomative cyclization to **223** when treated with a chiral palladium catalyst. Products were isolated in high yield and enantioselectivity; all examples possessed a quaternary carbon at C-10 and useful synthetic handles. After oxidative addition of palladium, nucleophilic substitution could occur at the *para*- or *ortho*-position. The observed regioselectivity was explained by the kinetic preference of nucleophilic substitution at the *para*- over the *ortho*-position.

Heteroatom substituents on the aromatic ring were well-tolerated, including methoxy and furan moieties (**223a-e**). Alkyl substituents *ortho*- to the hydroxy group of the phenol were also tolerated (**223h, j**) and extended alkyl chains could be installed at C-10 without a drop in *ee* (**223g**). Both 5- and 6-membered rings could be constructed in excellent yield (**223g, h**) but annulation of a 7-membered B-ring saw a significant drop in yield (**223i**). Additionally, a vinyl triflate was successfully employed, offering the possibility of utilizing functionalized cyclohexenes rather than bromobenzenes (**223f**). This methodology can be extremely useful for construction of quassinoid skeletons in a very efficient and enantioselective manner. It could be even more powerful if more highly oxygenated and functionalized precursors were tolerated.



Scheme 22 Enantioselective Palladium-Catalyzed Cyclization of Bromophenols

5. Selected Structure-Activity Relationships and Investigations of Biological Mechanism of Action

Within the last few years, several original research papers and in-depth reviews have been published discussing the

biological function and structure-activity relationship (SAR) of quassinoids; consequently, this topic is not covered in detail herein.^{48–50} In general, the α,β -unsaturated ketone in ring A, the C-15 ester side chain, and the tetrahydrofuran bridge are key contributors to bioactivity; however, the mechanism of action of different quassinoids likely diverges considerably, and specific targets have rarely been unambiguously linked to the biological properties observed in phenotypic assays. The lack of mechanistic understanding is clearly one of the main factors currently limiting the therapeutic potential of quassinoids. Another limitation is a broad general toxicity profile that might be due to unselective inhibition of protein biosynthesis or cellular signalling pathways.

Brusatol, for example, was found to exert strong anti-proliferative activity in multiple cell types through inhibition of the phosphoinositide 3-kinase (PI3K) protein kinase B (PKB, Akt) pathway. A biotin-conjugated brusatol derivative provided evidence that the PI3K γ and PI3K $\text{C}2\beta$ isoforms were the main targets in brusatol-sensitive cells such as Raji (Burkitt's lymphoma) and SU-DHL-4 (diffuse large B-cell lymphoma); however, proteins such as p53 and p73 were other potential targets.⁵¹ A series of C-3 amino acid-conjugated brusatol analogs were synthesized to improve ADME properties and reduce toxicity (**224–239**, Figure 2). Several of these derivatives, in particular the L-3- β -homoalanine conjugate **227**, demonstrated similar or higher efficacy against a panel of malignant cell lines paired with improved liver microsome stability and enhanced tolerability in mice upon IP administration.⁵² Compounds **224–227** had lower toxicity than brusatol (**7**) while maintaining sub-100 nM IC_{50} values in Raji cell line cytotoxicity assays, but analog **227** proved to be particularly attractive. In vivo, no lethality was observed with **227** at a dose of 5 mg/kg while brusatol showed a 25% death rate at that dose when administered IP. Doses of **227** of up to 10 mg/kg were tolerated, while brusatol was limited to below 5 mg/kg when dosed every other day in mice.

To determine if the activity of these analogs originated from a release of brusatol (**7**), non-cleavable derivatives connected through an ether bond (**236–239**) were synthesized and shown to be generally inactive, indicating that the main function of the amino acid conjugates was to serve as prodrugs even though such conjugates may retain some intrinsic activity.

Attempts to synthesize amino acid conjugates at the C-15 position also resulted in the accidental formation of compound **240** through an intramolecular etherification reaction. Analog **240** was found to be inactive in Raji cells, demonstrating the importance of the C-15 side chain in brusatol (**7**).⁵³ In addition to the synthetic analogs, naturally occurring quassinoids have also been found to influence the PI3K/Akt/NF- κB signalling pathway. Bruceoside B, in particular, inhibited Akt and showed promise as a therapeutic lead structure for acute lung injury in an in vivo lipopolysaccharide (LPS) model.⁹

Bruceantin (**6**), in contrast, was recently identified as a potent inhibitor of aberrant full-length androgen receptor (AR-FL) and its constitutively active variant 7 (AR-V7) in a cell-based

castration-resistant prostate cancer (CRPC) reporter assay. In this case, mechanistic evidence pointed toward the quassinoid binding to heat shock protein 90 (HSP90) and disrupting the HSP90 complex with AR-FL/AR-V7. Ultimately, bruceantin thus promoted the degradation of AR-FL/AR-V7 through the ubiquitin-proteasome pathway.⁵⁴

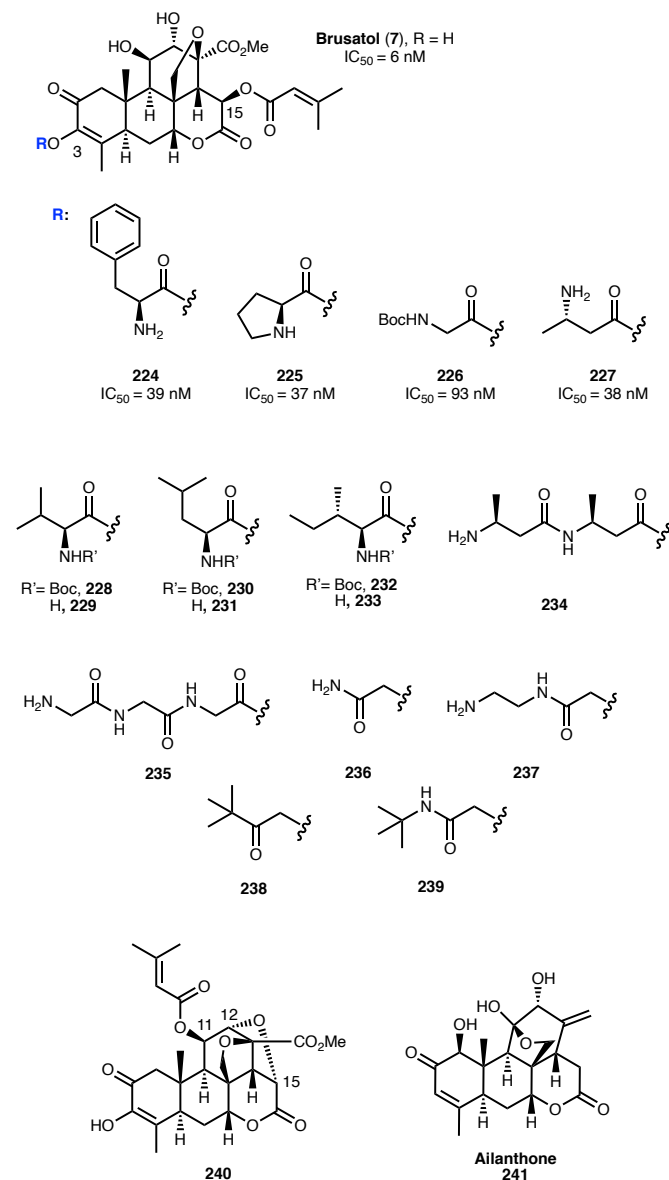


Figure 2 Selected Examples of Amino Acid Conjugates and Bis-Tetrahydrofuran Bridge Analog. IC₅₀ values for **7** and **224–227** refer to half-maximal inhibitory concentrations in Raji cells.⁵¹

Another major driver of oncogenesis, the signal transducer and activator of transcription-3 (STAT-3) pathway, was postulated as the target of ailanthone (**241**), a quassinoid extracted from the Chinese medicinal herb *Ailanthus altissima*. Cell based gene and protein expression studies served as evidence for an inhibition of the Janus kinase (JAK)/STAT-3 signalling pathway, but also suggested effects through caspase

and Bcl-2 family members. Irrespective of the mechanism of action of **241**, several quassinoids are attractive lead structures for the treatment of colorectal cancer (CRC).⁵⁵

6. Conclusions

Quassinoids display a wide range of biological activities and many of these natural products continue to offer significant opportunities for development as therapeutic agents. Moreover, quassinoids still pose attractive strategic and tactical synthetic problems. Chemists have already explored a multitude of creative approaches to construct the highly oxygenated polycyclic ring systems. As a result, advanced enantiomerically enriched intermediates have been synthesized in efficient and novel ways. Noteworthy recurring reactions in these approaches include the Diels–Alder and radical- or metal-mediated cyclizations. Future innovations might well be based on C,H-bond activations and photochemical transformations. Quassinoids would also represent very interesting targets for the investigation of advanced retrosynthetic artificial intelligence (AI) and machine-learning algorithms. Most likely, quassinoids will therefore continue to be the target of many synthetic adventures and a playground for innovative strategies.

A driving force for future research is clearly the still untapped therapeutic potential of these natural products. However, the latter will strongly depend on medicinal chemists' ability to elucidate the biological mechanism of action, correlate *in vitro* activity with cellular target engagement, and identify natural quassinoids or generate synthetic analogs with high target selectivity. We hope that the preparative tactics and strategies discussed in this review will help to enable the latter approach.

Author Contributions

Both EJP and PW contributed to the conceptualization and writing of the manuscript. The authors gratefully acknowledge financial support from DOD grant W81XWH-14-1-0117 (EJP, PW) and the Academy of Finland PROF16 program (PW).

Conflicts of interest

There are no conflicts to declare.

Notes and references

- J. Polonsky, in *Progress in the Chemistry of Organic Natural Products*, ed. W. Herz, H. Grisebach, G. W. Kirby, and Ch. Tamm, Springer, Vienna, 1st edn, 1985, Quassinoid Bitter Principles II, pp 221–264.
- J. Polonsky, in *Recent Advances of Phytochemistry*, ed. V.C. Runeckles and T.J. Mabry, Academic Press, New York, Vol 6, 1973, Chemistry and Biogenesis of the Quassinoids (Simaroubolides), pp 31–64.

- 3 W. Q. Yang, X. H. Shao, F. Deng, L. J. Hu, Y. Xiong, X. J. Huang, C. L. Fan, R. W. Jiang, W. C. Ye and Y. Wang, *J. Nat. Prod.*, 2020, **83**, 1674–1683.
- 4 B. Mendez, J. Reyes, I. Conde, Z. Ramos, E. Lozada, A. M. Cruz, G. Asencio, A. Carvajal, S. Dharmawardhane, D. M. Piñero-Cruz, E. Hernández, P. Vivas and C. A. Ospina, *Plants*, 2020, **9**, 93.
- 5 W. Q. Yang, W. Tang, X. J. Huang, J. G. Song, Y. Y. Li, Y. Xiong, C. L. Fan, Z. L. Wu, Y. Wang and W. C. Ye, *Molecules*, 2021, **26**, 5939.
- 6 C. He, Y. Wang, T. Yang, H. Wang, H. Liao and D. Liang, *J. Agric. Food Chem.*, 2020, **68**, 117–127.
- 7 J. J. Chen, W. Bai, Y. B. Lu, Z. Y. Feng, K. Gao and J. M. Yue, *J. Nat. Prod.*, 2021, **84**, 2111–2120.
- 8 W. Y. Zhao, X. Y. Song, L. Zhao, C. X. Zou, W. Y. Zhou, B. Lin, G. D. Yao, X. X. Huang and S. J. Song, *J. Nat. Prod.*, 2019, **82**, 714–723.
- 9 X. He, J. Wu, T. Tan, W. Guo, Z. Xiong, S. Yang, Y. Feng and Q. Wen, *Fitoterapia*, 2021, **153**, 104980.
- 10 S. Guo, J. Zhang, C. Wei, Z. Lu, R. Cai, D. Pan, H. Zhang, B. Liang and Z. Zhang, *Cancer Chemother. Pharmacol.*, 2020, **85**, 1097–1108.
- 11 N. Wei, J. Li, C. Fang, J. Chang, V. Xirou, N. K. Syrigos, B. J. Marks, E. Chu and J. C. Schmitz, *Oncogene*, 2019, **38**, 1676–1687.
- 12 Z. Q. Lai, S. P. Ip, H. J. Liao, Z. Lu, J. H. Xie, Z. R. Su, Y. L. Chen, Y. F. Xian, P. S. Leung and Z. X. Lin, *Front. Pharmacol.*, 2017, **8**, 936.
- 13 C. L. Wiseman, H. Y. Yap, A. Y. Bedikian, G. P. Bodey, and G. R. Blumenschein, *Am. J. Clin. Oncol.*, 1982, **5**, 389–391.
- 14 J. C. Arseneau, J. M. Wolter, M. Kuperminc and J. C. Ruckdeschep, *Investig. New Drugs*, 1983, **1**, 239–242.
- 15 M. Cuendet and J. M. Pezzuto, *J. Nat. Prod.*, 2004, **67**, 269–272.
- 16 M. Sasaki, T. Murae and T. Takahashi, *J. Org. Chem.*, 1990, **55**, 528–540.
- 17 J. M. Vanderroest and P. A. Grieco, *J. Am. Chem. Soc.*, 1993, **115**, 5841–5842.
- 18 P. A. Grieco, J. L. Collins, E. D. Moher, T. J. Fleck and R. S. Gross, *J. Am. Chem. Soc.*, 1993, **115**, 6078–6093.
- 19 (a) M. Kim, K. Kawada, R. S. Gross and D. S. Watt, *J. Org. Chem.*, 1990, **55**, 504–511. (b) N. Stojanac and Z. Valenta, *Can. J. Chem.*, 1991, **69**, 853–855. (c) E. D. Moher, J. L. Collins and P. A. Grieco, *J. Am. Chem. Soc.*, 1992, **114**, 2764–2765. (d) T. K. M. Shing, Q. Jiang and T. C. W. Mak, *J. Org. Chem.*, 1998, **63**, 2056–2057.
- 20 T. K. M. Shing and Y. Y. Yeung, *Angew. Chem. Int. Ed.*, 2005, **44**, 7981–7984.
- 21 T. K. M. Shing and Y. Y. Yeung, *Chem. Eur. J.*, 2006, **12**, 8367–8377.
- 22 Q. Jiang and T. K. M. Shing, *Tetrahedron Lett.*, 2001, **42**, 5271–5273.
- 23 W. P. Thomas and S. V. Pronin, *J. Am. Chem. Soc.*, 2022, **144**, 118–122.
- 24 D. J. Burns, S. Mommer, P. O'Brien, R. J. K. Taylor, A. C. Whitwood and S. Hachisu, *Org. Lett.*, 2013, **15**, 394–397.
- 25 S. Poigny, M. Guyot and M. Samadi, *J. Org. Chem.*, 1998, **63**, 5890–5894.
- 26 A. Dion, P. Dubé and C. Spino, *Org. Lett.*, 2005, **7**, 5601–5604.
- 27 C. Spino, *Synlett*, 2006, **1**, 23–32.
- 28 S. Perreault and C. Spino, *Org. Lett.*, 2006, **8**, 4385–4388.
- 29 A. Dion and C. Spino, *Heterocycles*, 2017, **95**, 894–919.
- 30 C. Spino, C. Thibault and S. Gingras, *J. Org. Chem.*, 1998, **63**, 5283–5287.
- 31 K. Usui, T. Suzuki and M. Nakada, *Tetrahedron Lett.*, 2015, **56**, 1247–1251.
- 32 Y. Oki and M. Nakada, *Tetrahedron Lett.*, 2018, **59**, 926–929.
- 33 A. Cervi, P. Aillard, N. Hazeri, L. Petit, C. L. L. Chai, A. C. Willis and M. G. Banwell, *J. Org. Chem.*, 2013, **78**, 9876–9882.
- 34 P. Y. Caron and P. Deslongchamps, *Org. Lett.*, 2010, **12**, 508–511.
- 35 K. Ravindar, P. Y. Caron and P. Deslongchamps, *Org. Lett.*, 2013, **15**, 6270–6273.
- 36 K. Ravindar, P. Y. Caron and P. Deslongchamps, *J. Org. Chem.*, 2014, **79**, 7979–7999.
- 37 F. A. Macías, J. M. Aguilar, J. M. G. Molinillo, F. Rodríguez-Luís, I. G. Collado, G. M. Massanet and F. R. Fronczek, *Tetrahedron*, 2000, **56**, 3409–3414.
- 38 I. S. Marcos, N. García, M. J. Sexmero, F. A. Hernández, M. A. Escola, P. Basabe, D. Díez and J. G. Urones, *Tetrahedron*, 2007, **63**, 2335–2350.
- 39 I. S. Marcos, B. Martínez, M. J. Sexmero, D. Diez, P. Basabe and J. G. Urones, *Synthesis*, 2006, **22**, 3865–3873.
- 40 V. Cwynar, M. G. Donahue, D. J. Hart and D. Yang, *Org. Lett.*, 2006, **8**, 4577–4580.
- 41 D. J. Hart and D. Yang, *Heterocycles*, 2007, **73**, 197–201.
- 42 D. Yang, V. Cwynar, M. G. Donahue, D. J. Hart and G. Mbogo, *J. Org. Chem.*, 2009, **74**, 8726–8732.
- 43 M. G. Donahue and D. J. Hart, *Can. J. Chem.*, 2004, **82**, 314–317.
- 44 K. Hung, X. Hu and T. J. Maimone, *Nat. Prod. Rep.*, 2018, **35**, 174–202.
- 45 M. L. Condakes, R. Z. Rosen, S. J. Harwood and T. J. Maimone, *Chem. Sci.*, 2019, **10**, 768–772.
- 46 E. E. Robinson and R. J. Thomson, *J. Am. Chem. Soc.*, 2018, **140**, 1956–1965.
- 47 K. Du, P. Guo, Y. Chen, Z. Cao, Z. Wang and W. Tang, *Angew. Chem. Int. Ed.*, 2015, **54**, 3033–3037.
- 48 Z. K. Duan, Z. J. Zhang, S. H. Dong, Y. X. Wang, S. J. Song and X. X. Huang, *Phytochemistry*, 2021, **187**, 112769.
- 49 Z. Li, J.-Y. Ruan, F. Sun, J.-J. Yan, J.-L. Wang, Z.-X. Zhang, Y. Zhang and T. Wang, *Chem. Pharm. Bull.*, 2019, **67**, 654–665.
- 50 G. Fiaschetti, M. A. Grotzer, T. Shalaby, D. Castelletti and A. Arcaro, *Curr. Med. Chem.*, 2011, **18**, 316–328.
- 51 Y. Pei, N. Hwang, F. Lang, L. Zhou, J. H. Y. Wong, R. K. Singh, H. C. Jha, W. S. El-Deiry, Y. Du and E. S. Robertson, *Commun. Biol.*, 2020, **3**, 267.

Journal Name

ARTICLE

- 52 N. Hwang, Y. Pei, J. Clement, E. S. Robertson and Y. Du, *Bioorganic Med. Chem. Lett.*, 2020, **30**, 127553.
- 53 K. E. Crocker, Y. Pei, E. S. Robertson, J. D. Winkler and Y. Pei, *Can. J. Chem.*, 2020, **98**, 270–272.
- 54 S. J. Moon, B. C. Jeong, H. J. Kim, J. E. Lim, H.-J. Kim, G. Y. Kwon, J. A. Jackman and J. H. Kim, *Theranostics*, 2021, **11**, 958–973.
- 55 H. Ding, X. Yu and Z. Yan, *Int. J. Mol. Med.*, 2022, **49**, 21.